




# A simplified numerical model to simulate RC beam–column joints collapse

Javad Shayanfar<sup>1</sup> · Ali Hemmati<sup>1</sup> · Habib Akbarzadeh Bengar<sup>1</sup> 

Received: 10 March 2018 / Accepted: 11 September 2018 / Published online: 22 September 2018  
© Springer Nature B.V. 2018

## Abstract

Post-earthquake reconnaissance confirmed that the high vulnerability of non-seismically detailed RC frame structures could be related to shear failure in the core of the beam–column joints which might cause the collapse of the structure. The main focus was given on developing a simplified numerical model to simulate RC beam–column joints collapse based on theoretical formulations and experimental observations. For this, a joint model has been proposed so that nonlinearities in the joint core were considered by two diagonal axial springs. According to the principal stress approach, a more refined calibration of principle tensile stress versus joint rotation relation was developed to calculate the characteristics of these springs. In the model, the effects of the main factors influencing the mechanical behavior of RC joints i.e. column intermediate bars, joint aspect ratio, joint shear reinforcements, type of beam bar anchorage, etc. were considered. To verify the simplified numerical model, it was vastly applied to experimental specimens available in the literature. Results revealed that the model was capable of estimating inelastic response of RC joints with reasonable precision. Furthermore, assuming the joint core to behave as a rigid body, even for joints reinforced by shear reinforcements might bring about non-conservative predictions in terms of strength and ductility capacities. Based on a parametric study, it was also concluded that the effectiveness of the influential factors of RC beam–column joints is noticeably a function of the level of the axial load applied on the column. Using experimentally computed factors and simple procedure to calculate joint characteristics could make the model properly suitable for practical applications.

**Keywords** Beam–column joint · Nonlinear analysis · Principal tensile stress · Simplified numerical model

## 1 Introduction

Post-earthquake reconnaissance confirmed the high vulnerability of non-seismically detailed reinforced concrete (RC) frame structures, with emphasis on poor performance of the beam–column joints. Indeed, due to inadequately designed shear reinforcements in the

---

✉ Habib Akbarzadeh Bengar  
h.akbarzadeh@umz.ac.ir

<sup>1</sup> Department of Civil Engineering, University of Mazandaran, Babolsar, Iran

joint core, being designed merely for gravity loads (lack of a capacity design principles) and improper seismic specific details (insufficient anchorage length, short lap splices and discontinuous longitudinal bars), non-seismically detailed joints are highly likely to be vulnerable to shear or bond failure, especially in seismic prone area. To improve seismic performance of RC joints, several retrofitting techniques such as removal and replacement, RC jacketing, steel jacketing, haunch retrofit solution (HRS), epoxy repair, steel fibers and fibre reinforced polymers (FRP) bonding have been analytically and experimentally studied and used in practical applications. However, prior to following each retrofitting technique, the determination of the seismic response of RC joints in terms of failure mode, strength and ductility is of paramount importance. Many investigations have been conducted to evaluate inelastic response of RC joints and to appropriately review these studies, they were categorized into three groups, experimental, numerical, and analytical studies.

In the group of experimental investigations, Genesio and Sharma (2010) tested exterior non-seismic RC beam–column joints with various beam bar anchorages. It was found that joint failure mechanism could be noticeably a function of the type of beam bar anchorage. It has also been confirmed by experimental studies (Pantelides et al. 2002; Hertanto 2005; Parvin et al. 2010; Melo et al. 2012; Sharma 2013; Shafaei et al. 2014). Kaung and Wong (2013) investigated the effectiveness of horizontal stirrups in the joint core on the seismic performance and shear strength of the non-ductile RC joints. The results showed that horizontal shear reinforcements effectively improved seismic behavior and considerably enhanced joint shear strength.

In the group of numerical investigations, Niroomandi et al. (2014) carried out a numerical parametric study on non-seismic RC beam–column joints with various beam longitudinal bar and joint aspect ratios. It was concluded that these parameters could noticeably overwhelm the joint nonlinear behavior. Del Vecchio et al. (2016) conducted a numerical seismic assessment of RC structural systems designed without proper seismic details in the joint core. A new modelling strategy was developed to account for the joint nonlinear behavior in the finite element method. A mechanical model was also proposed to consider the effect of beam longitudinal bar anchorages on the seismic response of the joint core. Genesio (2012) dealt with a numerical parametric study through finite element analysis to simulate non-ductile exterior joints. The influential factors, such as beam and column bar ratio, the compressive strength of concrete  $f'_c$ , column axial force and joint aspect ratios, on joint behavior in terms of principal tensile stress, were scrutinized. It was found that the increase of joint shear capacity tend to be linearly proportional to  $\sqrt{f'_c}$ ; Column longitudinal ratios marginally influences principle tensile stresses corresponding to the peak load and first diagonal cracking, respectively; The joint geometric aspect ratio can significantly overwhelm the joint shear strength; Increasing axial load level on the column, maximum principle tensile stress and joint shear capacity would generally decrease and increase, respectively.

Finally, in the group of analytical studies, several beam–column joint models, consisting of various types of springs i.e. axial or/and shear or/and rotational springs have been proposed for simulating nonlinearities in the joint core as well as beam and columns (Pamparin et al. 2003; Lowes and Altoontash 2003; Wong 2005; Favvata et al. 2008; Niroomandi et al. 2010; Sharma et al. 2011; Unal and Burak 2013; Jeon et al. 2015; Shayanfar et al. 2016; De Risi et al. 2016a, b; Shayanfar et al. 2017; Shayanfar and Akbarzadeh 2018, Shayanfar et al. 2018). A beam–column joint model, containing a zero length rotational spring as well as rigid links to define the joint panel geometry, was proposed by Pamparin et al. (2003). The rotational spring characteristics were determined through principal tensile stress- shear deformation relation in the joint core. Sharma et al. (2011) followed a

similar approach, but the joint model was included a flexural spring and two shear springs to account for nonlinearities in the joint core. Shayanfar et al. (2016) came up with a joint model with two diagonal axial springs in the joint core, in which the spring characteristics were calculated based on principal tensile stress-shear deformation relation depending the type of beam bar anchorage. It is worth notifying that an incremental procedure was proposed to calculate shear reinforcement contribution on maximum principal tensile stress in the joint core using a combination of a mechanically-based model and empirical observations.

Even though several beam–column joint models have been recommended, despite of their effectiveness, a simple and generalized formulation, to be suitable for following in practical applications of RC joints with various beam bar anchorages and joint shear reinforcement ratios, seems to be needed. Difficulties in the definition of the beam–column joint model arise when the main factors influencing the mechanical behavior of RC joints are considered. The RC joint response noticeably depends on several factors such as the axial load level, column intermediate reinforcements, beam longitudinal bars, concrete compressive strength, joint aspect ratio, the ratio of beam depth to beam width, joint shear reinforcements, the type of beam bar anchorage, joint failure mechanism, etc. To studiously overcome the challenges of definition of the exact nonlinear behavior of RC beam–column joint, empirical equations along with simplified procedures to approximately predict the principal tensile stress in the joint core can be developed using a large database of test results and considering the mentioned influential factors. This approach has been recently followed by Genesio (2012), Sharma (2013), Shayanfar et al. (2016) and Shayanfar and Akbarzadeh (2016). In this paper, according to the principal stress approach, a more refined calibration of principle tensile stress versus joint rotation relation was developed to calculate inelastic behavior of corner RC beam–column joints. Accordingly, based on an extended set of results of experimental and finite element studies on RC joints with various beam bar anchorage types, available in literature, classified by the joint main parameters, a refined analytical joint model was addressed in the paper. Ultimately, the simple analytic approach and using experimentally calculated factors are prone to making the developed model sufficiently suitable in practice.

## 2 Modelling approach

According to the poor performance of the beam–column joints in existing RC structures, considering nonlinearities merely in the beam/column members along with the conventional assumption of the rigid behavior for the joint core element is highly likely to cause misleading results, especially for non-conforming joints. It is because that for RC structures, especially old buildings designed without using the prescriptions of modern seismic provision, seismic response could be controlled by brittle failure in the joint core. In the present study, the numerical model developed Shayanfar et al. (2016) containing two diagonal axial springs in the joint core, which is capable of being implemented in commercial softwares, was followed as shown in Fig. 1.  $L_b$  and  $L_c$  define the beam length measured from the column face and the total column height, respectively (the other parameters were defined in the figure). As can be observed in the figure, in addition to axial springs, some rotational springs were considered in beam and column elements. The mechanism of nonlinear behavior of an RC exterior beam–column joints under seismic actions was illustrated in Fig. 2.  $V_{jh}$  and  $V_{jv}$  define the horizontal and vertical joint shear forces, respectively (the

**Fig. 1** Numerical model for an RC FRP strengthened joint

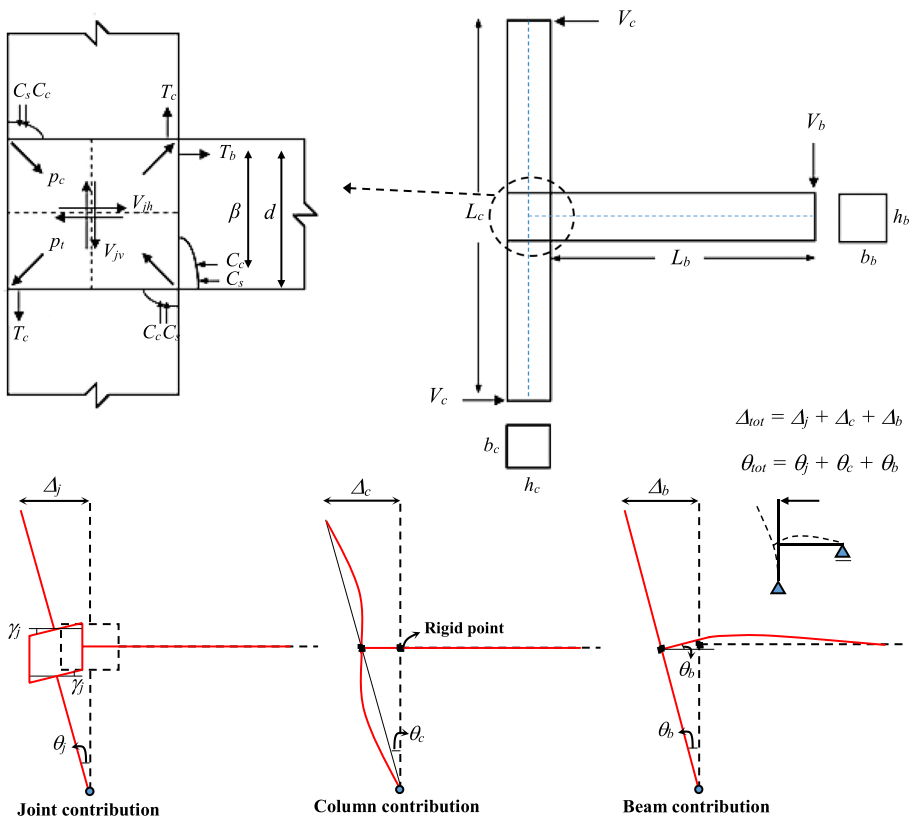
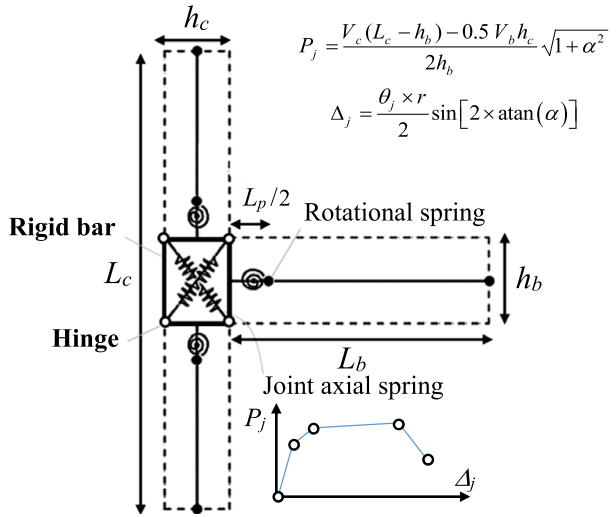


**Fig. 2** Mechanics of an RC beam–column joint subjected to lateral loading

other parameters were defined in the figure). As can be seen in the figure, the total horizontal rotation/displacement are composed of the horizontal rotations/displacements induced by the deformation of the joint core, beam and column. Accordingly, simulating nonlinearities in each component using the assigned springs, nonlinear behavior of the beam–column joint could be determined.

To generate the characteristics of joint axial springs, the principal tensile stress due to concrete and shear reinforcements corresponding to the joint rotation can be converted into diagonal axial force versus displacement relation. After the determination of beam/column element characteristics, nonlinear analysis can be performed to simulate the seismic response of RC joints. This approach is also proper for modelling beam–column joints at the structural level through commercial softwares in compliance with lumped plasticity approach or simplified seismic evaluation procedures i.e. Del Vecchio et al. (2017).

### 3 Determination of the characteristics of diagonal axial springs

In this section, the procedure to calculate the nonlinear characteristics of diagonal axial springs, which can be used in nonlinear static analyse (pushover) with modelling the joint core, will be addressed. It should be noted that from the point of view of seismic assessment of RC structures, nonlinear dynamic analyses have been recognized as the most accurate ones. Accordingly, in the case of developing a joint element model taking into account strength and stiffness degradation hysteresis rules, including the case of pinching effect, is of paramount importance. However, it should be considered that nonlinear dynamic analysis can be highly prohibitive in terms of computational efforts and time required to comprehensively carry out a nonlinear dynamic analysis. Therefore, in the current study, the focus has been on developing a simplified and accurate beam–column joint model to be followed in nonlinear static analyses due to the fact that it can be more practical than nonlinear dynamic analyses for most engineers.

According to the mechanism of nonlinear behavior of an RC exterior beam–column joints under seismic actions as illustrated in Fig. 2, through the internal equilibrium in joint core, the column shear force,  $V_c$ , was derived as:

$$V_c = T_b - V_{jh} \tag{1}$$

where  $T_b$  = the tensile force in beam longitudinal reinforcements; Using the external equilibrium in the beam–column joint, the beam shear force,  $V_b$ , can be written as:

$$V_b = V_c \frac{L_c}{L_b + 0.5h_c} \tag{2}$$

Substituting Eq. (2) into Eq. (1), we have:

$$V_b \frac{L_b + 0.5h_c}{L_c} = \frac{V_b L_b}{\beta} - V_{jh} \tag{3}$$

where  $\beta$  = the ratio of the beam moment to the beam tensile force at the column face. Rearranging Eq. (3),  $V_b$  can be derived as:

$$V_b = \frac{\beta \xi_e}{(\xi_e - \beta) L_b} V_{jh} \tag{4}$$

in which

$$\xi_e = \frac{L_c L_b}{L_b + 0.5 h_c} \quad (5)$$

To calculate the exact value of  $\beta$  corresponding to horizontal joint shear force as well as beam shear force, an iterative procedure might be required as proposed by Sharma et al. (2011) and Shayanfar et al. (2016). However, in the present study, for simplicity, it was considered  $0.9d$  (Akguzel and Pampanin 2012). In the present study, to transform  $V_b$  and  $V_c$  corresponding to  $V_{jh}$  and joint rotation,  $\theta_j$ , into diagonal axial force versus displacement relationship to be used in the determination of the diagonal axial spring characteristics, the equations proposed by Shayanfar et al. (2016), which was compatible to the commercial software SAP2000 (2008) were adopted. Accordingly, the diagonal axial force and corresponding displacement can be calculated as:

$$P_j = \frac{V_c(L_c - h_b) - 0.5V_b h_c}{2h_b} \sqrt{1 + \alpha^2} \quad (6a)$$

$$\Delta_j = \frac{\theta_j \times r}{2} \sin(2 \times \text{atan}[h_b/h_c]) \quad (6b)$$

where  $\alpha$  and  $r$  = the joint geometric aspect ratio and the length of diagonal of the joint core. The other parameters were already defined in Fig. 2.

The principal stress approach consists of evaluating the average stress produced in the joint core during seismic actions and compares the resulted principal stresses with certain critical values, as damage index. These values of allowable stress have been recommended for different limit states i.e. joint cracking and ultimate capacities. Due to its simplicity in application, it has been followed in various design codes i.e. NZS 3101 (1995), ACI 352 (2002) etc., where the average horizontal shear stress in the joint core is compared to the allowable stresses. Accordingly, in this study, due to the fact that this approach considers  $V_{jh}$  corresponding to axial compressive stress on column,  $f_v$ , entering in the joint core in a sufficiently practical way. It would be also proper to present an appropriate understand and a rational basis of calculating  $V_{jh}$ . As a result, the approach suggested by Priestley (1997) according to Mohr's theory was adopted as:

$$p_{t,tot} = \sqrt{\left(\frac{f_v}{2}\right)^2 + \left(\frac{V_{jh}}{b_j h_c}\right)^2} - \frac{f_v}{2} \rightarrow V_{jh} = \left(\sqrt{1 + \frac{f_v}{p_{t,tot}}}\right) p_{t,tot} b_j h_c \quad (7)$$

where  $b_j = (b_b + b_c)/2$  (Park and Mosalam 2012);  $p_{t,tot}$  = the principal tensile stress contributions due to concrete and stirrup. In the following, the focus was given on predicting  $p_{t,tot}$  based on regression analysis. For this, a large database including 390 test results and specimens generated by finite element analyses of exterior RC beam–column joints with shear/bond failure in the joint core was provided whose details can be found in Appendix Table 2. In Table 1, statistics consisting of minimum, maximum, mean, and coefficient of variation (COV) for important parameters were presented.  $\rho_b$  = the beam bar ratio;  $r_N$  = the level of axial load applied on the column ( $N/A_j \times f'_c$ );  $S_j$  = the joint shear reinforcement index ( $S_j = A_{sx} \times f_{ys} \times \sin(\text{atan}[h_b/h_c]) / A_j \times f'_c$ ), based on Shayanfar and Akbarzadeh (2018).  $A_{sx}$  and  $f_{ys}$  = total area of joint shear reinforcements and their yield strength, respectively.

It should be noted that 103 specimens were generated by finite element analyses carried out by Genesio (2012) (the finite element model was appropriately calibrated by the

**Table 1** Summary of the details of the test results and specimens generated by finite element analyses

Statistics	$f'_c$	$b_b$	$h_b$	$b_c$	$h_c$	$\rho_b$	$S_f^a$	$\alpha$	$r_N$
Min	8.05	100	180	100	150	0.0026	0.003	0.89	-0.04
Max	101.6	610	610	650	520	0.0209	0.162	2.00	0.47
Mean	30.9	250	370	276	275	0.0082	0.044	1.37	0.08
COV	0.419	0.312	0.244	0.320	0.276	0.453	0.741	0.175	1.052

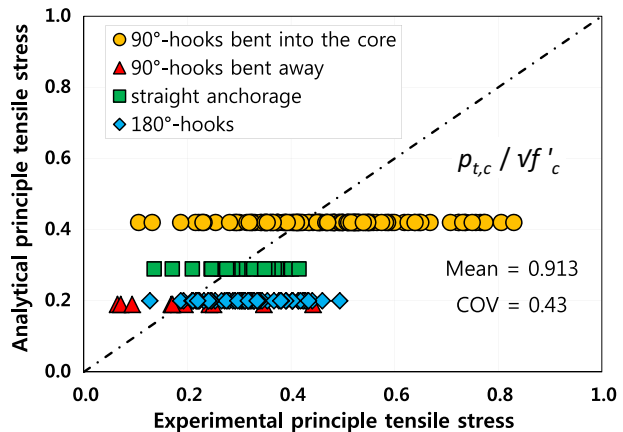
<sup>a</sup>Based on the test specimens with shear reinforcements

experimental studies conducted by Hertanto 2005 and Genesio and Sharma 2010) and other ones were conducted in laboratories. Furthermore, 133 specimens were RC joints with shear reinforcements (test specimens with shear failure in the joint core were only chosen) and others were not reinforced.

According to experimental evidence, the limit states for principal tensile stress as a function of concrete compressive strength have been suggested by Priestly (1997), Sharma et al. (2011) and Akguzel and Pampanin (2012) for joints with 90°-hooks bent into (0.42√f'\_c), 90°-hooks bent away (0.29√f'\_c), short embedded length (0.19√f'\_c) and 180°-hooks (0.2√f'\_c). These limit states were compared to the results obtained from test specimens available in literature (with no shear reinforcement in the joint core) to evaluate their reliability (Fig. 3). Considering the values of the mean, mean absolute percentage error, MAPE, and COV, the limit states do not seem to be capable of precisely predicting the joint response, even though they present the merits of being quite simple and efficiently practical. According to test results and specimens generated by finite element analyses, Genesio (2012) recommended the limit states to calculate first diagonal crack and maximum principle tensile stresses considering the influential effects of several factors i.e. concrete compressive strength, amount and detailing of beam longitudinal bars, axial load level and joint aspect ratio.

Likewise, Sharma (2013) suggested that according to the experimental study conducted by Wong and Kuang (2008) highlighting the significant effect of joint aspect ratio on principal tensile stress, its critical values can be divided by the factor α. Accordingly, the principal

**Fig. 3** Comparison of the results obtained from experiments and existing models



tensile stress does not seem to be influenced by just concrete compressive strength, while the effects of factors of joint aspect ratio ( $\alpha$ ), the level of the axial load ( $r_N$ ), joint shear reinforcement index ( $S_j$ ), the ratio of beam depth to beam width ( $h_b/b_b$ ), and amount and detailing of beam longitudinal bars ( $r_B$ ) might be crucially noticeable as shown in Fig. 4.

It is noteworthy that joint capacity would be influenced by a combination of the effects of these important factors and the figure can be useful to assess their general effects. As can be seen in the figure, increasing  $S_j$  and  $r_B$ , principle tensile stress would considerably increase. On the contrary, axial load level might negatively influence principle tensile stress. However, the experimental principle tensile stresses seem to be variable increasing  $\alpha$  and  $h_b/b_b$ , although the trends reveal that  $p_t/\sqrt{f'_c}$  insignificantly decrease increasing these parameters, especially for joints with 90°-hooks bent away from the core and 180°-hooks.

For an RC beam–column joint, increasing the joint geometric aspect ratio, the concrete strut angle with horizontal would be higher and the horizontal component of the concrete strut resisting tensile force in beam longitudinal reinforcements should, subsequently, be less. Therefore, more compression force in the diagonal strut would be needed to maintain equilibrium, for same tensile force. Accordingly, due to the enhanced demand in the diagonal strut, shear capacity in the joint region could decrease. The tension force in beam longitudinal reinforcements caused by bending moment at the face of the column is transferred into the joint region through the bond mechanism as well as the mechanical anchorage at the end of the beam longitudinal reinforcements. Considering the joint shear failure corresponding to the strut failure which starts at the beam longitudinal reinforcement anchorage, it can be argued that increasing beam bar ratio and subsequently, an increase in the component of tensile forces transferred by bond mechanism, the concrete diagonal strut failure would occur at a higher strength. Furthermore, increasing  $\rho_b$ , the bending of the beam longitudinal reinforcement becomes more effectual in supporting the diagonal strut (Genesio 2012). As can be seen in Fig. 4, principle tensile stress seems to be negatively influenced increasing  $r_N$ . However, it is worth noting that the axial load is capable of improving joint shear strength (Clyde et al. 2000; Pantelides et al. 2002; Wong 2005; Pampanin et al. 2007; Parvin et al. 2010; Genesio 2012) so that it can increase the compression demand in the concrete strut, whereas its width enhances by the expansion of the compression zone in the end of the column, simultaneously. Likewise, increasing axial load level, tensile strains in column longitudinal reinforcements would be reduced so that it could delay flexural yielding of the column as well as column bar yield penetration into the joint region. Accordingly, it would bring about an increase in joint strength.

In the current study, in light of these discussions, according to the provided database, using nonlinear regression, the principal tensile stress contributions due to concrete and shear reinforcements corresponding to maximum joint horizontal shear strength can be calculated as:

$$p_{t,tot} = p_{t,c} + p_{t,s} = \frac{\omega_{CR}\omega_{BA}}{\omega_{setup}} \omega_S \omega_1 \sqrt{f'_c} \quad (8)$$

in which

$$\omega_1 = 0.25X^{1.3} + 0.2 \quad (9)$$

$$X = \left(1 + S_j^{0.26}\right) \left(1 + r_N^{0.48}\right) f'_c{}^{0.31} r_B^{0.45} \alpha^{-0.18} \left(\frac{h_b}{b_b}\right)^{0.4} \quad (10)$$



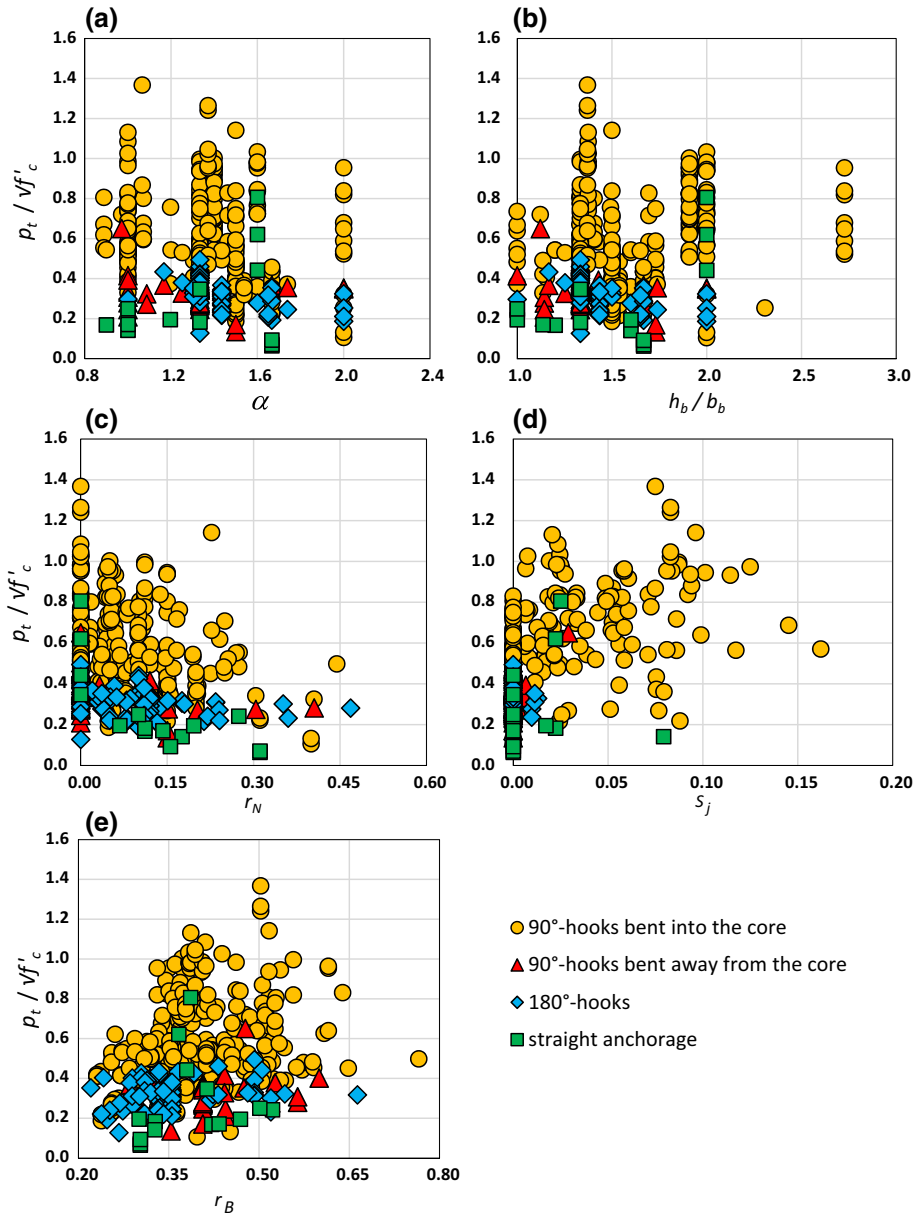


**Fig. 4** Variations of experimental principle tensile stress in the joint core according to the geometry and material properties in experimental RC joints: **a** joint aspect ratio; **b** the ratio of beam depth to beam width; **c** axial load level; **d** joint shear reinforcement index; **e** beam reinforcement index

where  $S_j$  was defined to introduce joint shear reinforcements in the joint core, based on Shayanfar and Akbarzadeh (2018);  $\omega_{BA}$ =the coefficient of the anchorage type of beam longitudinal bars.  $\omega_{CR}$ =the coefficient of the intermediate longitudinal reinforcement.  $\omega_{setup}$ =the coefficient of the beam–column joint test setup.  $\omega_s$ =the coefficient to consider

the effect of joint shear reinforcements on concrete contribution in maximum principal tensile stress. Generally, two different setups have been adopted for conducting experimental studies on exterior RC joints in which (1) a concentrated load ( $V_b$ ) was considered to be vertically applied at the end of the beam, while the ends of the column was considered to be hinged (type A); (2) the end of top column was loaded horizontally,  $V_c$ , so that could freely move in the horizontal direction, whereas the ends of bottom column and beam were hinged (type B). Despite the fact that the static of these systems in both test setups are quite identical, the shape of deformation are different altogether. It is noteworthy that the results which are extracted from experiment studies on RC beam–column joints (i.e. principle tensile stress and joint shear strength) are generally considered identical for both the test setups. However, according to the finite element study carried out by Genesio (2012), the characteristics of an RC beam–column joint would be overwhelmed by the test setup type. Considering this influential effect, the factor  $\omega_{setup}$  was, therefore, defined to transform results extracted from one test setup to another. In the present study,  $\omega_{setup} = 1.18$  (Genesio 2012) was adapted for converting joint characteristics with type A into type B. It is noted that since the boundary conditions and deformation shape in the type B seem to be closer to the reality of deformation of an RC joint at the structural level, for modelling RC joints at the structural level, in the calculation of the characteristics of the joint core,  $\omega_{setup} = 1.18$  should be followed.

Experimental and analytical studies (Priestley 1997; Pampanin et al. 2002; Murty et al. 2003; Wong 2005; Akguzel and Pampanin 2010; Hassan 2011; Sharma 2013; Shafaei et al. 2014; Shayanfar et al. 2016; De Risi and Verderame 2017) confirmed that failure mechanism and subsequently, the seismic response of RC joints noticeably depend on the type of beam bar anchorage as shown in Fig. 5.

As can be observed in Fig. 5a, for RC beam–column joints with 90°-hooks bent into, as the diagonal struts would be stabilized, after occurring the first diagonal cracking, the joint core would resist more and a hardening behavior could be, consequently, expected to occur in this region by the stage in which principal tensile stress in the joint region reaches its maximum value corresponding to more severe diagonal cracks.

For RC beam–column joints with 180°-hooks, as it is clear in the Fig. 5b, the failure mechanism is quite different from those with 90°-hooks bent in so that after forming the first diagonal cracking, joint behavior would lead to a “concrete wedge” brittle failure mechanism (Pampanin et al. 2002), due to the interaction between diagonal shear cracks and stress concentration at the location of the hook anchorage (Fig. 5b). Accordingly, maximum joint capacity can be reasonably expected to occur corresponding to first diagonal cracking in the joint core. Again, for RC beam–column joints with 90°-hooks bent away from joint region, the failure mechanism is approximately identical to those with 180°-hooks. In this type of the beam bar anchorage of joints, owing to the fact that the first shear cracking propagates along the beam longitudinal bars as well as because of the lateral thrust, the column cover could be fractured (Fig. 5c). Therefore, the diagonal concrete struts in the joint core cannot have an opportunity to be stabilized and the joint failure is, subsequently, expected at early stage in comparison with RC joints with beam longitudinal bars bent in. It might be because that in joints with 90°-hooks bent away or 180°-hooks, an effective node to active and develop the diagonal compression strut cannot be fully provided. In case of RC beam–column joints in which beam longitudinal bars terminates in the joint region with a short development length, the bond mechanism between concrete and beam longitudinal bars becomes a critical factor. The crack starts at the end of the anchorage, approximately at the column mid-depth as shown in Fig. 5d. It might trigger the bond failure much prior to fully developing the diagonal compressive strut mechanism. Accordingly, maximum joint strength can be expected to occur lower than that

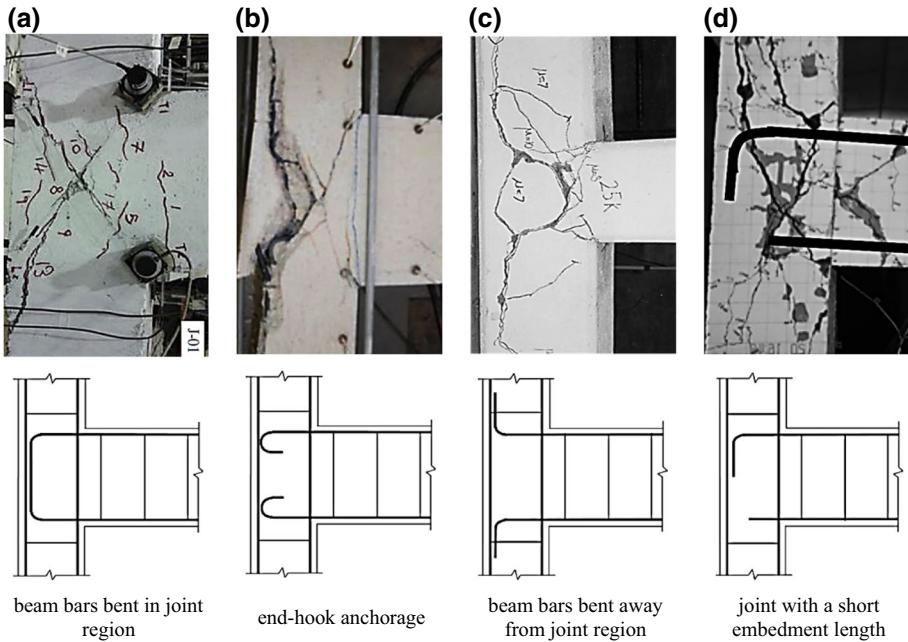


**Fig. 5** Failure mechanisms of RC joints based on the experimental studies conducted by **a** Realfonzo et al. (2014); **b** Ricci et al. (2016) **c** Gergely et al. (2000); **d** Genesio and Sharma (2010)

of RC joints with 90°-hooks bent in. In the present study, according to the examination of test specimens collected in the database, to consider the influential effect of the anchorage type of beam longitudinal bars,  $\omega_{BA}$  was defined which is equal to  $\omega_{BA}=0.82$  and  $0.61$  for RC joints with 180°-hooks and 90°-hooks bent away, respectively. For joints with straight anchorage, it is assumed that since the response of this type of the anchorage significantly depends on the development length of beam bars, increasing this length, the joint core tends to behave similar to joints with 90°-hooks bent into and subsequently, joint shear capacity becomes the critical parameter rather than bond mechanism between concrete and beam bars. In addition to the development length, Hassan (2011) suggested that bond mechanism also depends on the level of axial load and beam bar diameter. Accordingly, based on experimental studies,  $\omega_{BA}$  as a function of the development length of beam bars, axial load and beam bar diameter can be calculated by:

$$\begin{aligned} \omega_{BA} &= 0.75 \times \psi_s (1 + r_N^2) \left( \frac{L_d}{h_c - c'} \right) \\ &\approx 0.75 \times \psi_s (1 + r_N^2) \left( \frac{L_d}{0.93h_c} \right) \approx 0.806 \times \psi_s \frac{L_d}{h_c} (1 + r_N^2) \leq 0.9 \end{aligned} \tag{11}$$

where  $\psi_s=1$  for bar diameter  $\geq 19$  mm and  $\psi_s=1.2$  for bar diameter  $< 19$  mm (Hassan 2011).

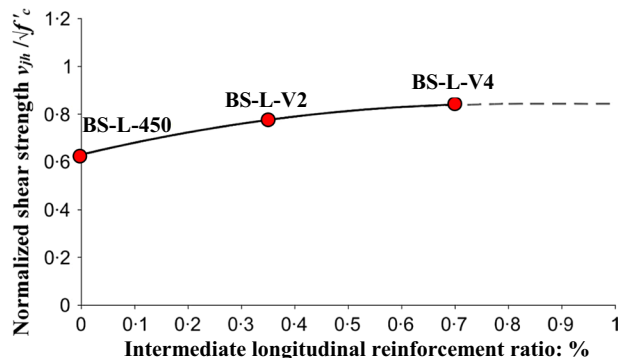
According to the finite element study conducted by Genesio (2012), it was found that there is a marginal difference in the ultimate capacity of RC joints for variable column longitudinal reinforcement ratios. Likewise, the joint shear deformation was inconsiderably influenced by

the variations of this factor. On the basis of this study, it could be assumed that the joint shear strength is independence on column longitudinal reinforcement ratios. However, it is noteworthy that in the all numerical specimens generated by Genesio (2012), there was not any column intermediate longitudinal reinforcement. On the other hand, experimental studies (Kaku and Asakusa 1991; Tsonos et al. 1992; Karayannis et al. 1998; Wong 2005; Wong and Kuang 2008; Chalioris et al. 2008) confirmed that intermediate longitudinal reinforcements are capable of considerably enhancing shear strength and effectually improving the hysteretic behavior of an RC beam–column joint. Figure 6 shows the results of the tests conducted by Wong and Kuang (2008) on the joint specimens with various column intermediate reinforcement ratios. As can be observed, the joint capacity can be influenced increasing column intermediate reinforcements so that the specimens of BS-L-V2 and BS-L-V4 experienced 24 and 33% growth in shear strength corresponding to intermediate longitudinal steel ratio of 0.35% and 0.7%, respectively. In this study, according to the studies of Kaku and Asakusa (1991), Tsonos et al. (1992), Karayannis et al. (1998), Wong (2005), Wong and Kuang (2008) and Chalioris et al. (2008), the coefficient of  $\omega_{CR}$  was used to consider the effect of the column intermediate longitudinal reinforcements on maximum principle tensile stress. To be conservative and simple, for all range of column intermediate reinforcement ratio,  $\omega_{CR}$  was assumed equal to 1.15.

As it was discussed, for RC beam–column joints, except joints with 90°-hooks bent into, the effective node point would not be provided in the joint core to develop diagonal compression strut mechanism. According to experimental studies (Tsonos et al. 1992; Karayannis et al. 1998; Murty et al. 2003; Wong 2005; Hwang et al. 2005; Wong and Kuang 2008; Chalioris et al. 2008; Kuang and Wong 2013; Kim et al. 2016), shear reinforcements in the joint core are prone to improving the joint capacity and also changing in failure mechanism if adequate shear reinforcements in the joint core were used. Hence, the joints would fail similar to joints with 90°-hooks and more severe diagonal cracking and damage in the joint core can be expected (Fig. 5). Accordingly, for joints with 90°-hooks bent out, 180°-hooks and straight anchorage, the concrete contribution of principle tensile stress might be enhanced by using shear reinforcements in the joint core. If the effective node points might be perfectly provided for developing diagonal compression strut mechanism,  $\omega_{BA} = 1$  could ideally be assumed. As a result, according to Eq. (8), principal tensile stress corresponding to maximum joint horizontal shear strength can be rewritten as:

$$P_{t,t} = \frac{\omega_{CR}\omega_{BA}}{\omega_{setup}} \omega_1 \sqrt{f'_c} \left[ \frac{1 - (1 - \omega_{BA})(1 - \psi)}{\omega_{BA}} \right] \quad (12)$$

**Fig. 6** Variations of joint shear capacity to column intermediate longitudinal reinforcement ratio (adopted from Wong and Kuang 2008)



where  $\psi$  = the coefficient to consider the improvement in the shear capacity due to joint shear reinforcements which was assumed equal to 15%. Accordingly, maximum principal tensile stress can be calculated as:

$$p_{t,tot} = \frac{\omega_{CR}}{\omega_{setup}} \omega_1 (0.15 + 0.85\omega_{BA}) \sqrt{f'_c} \tag{13}$$

where  $\omega_{CR} = 1.15$  and 1 for RC joints with and without column intermediate reinforcements. It should be noteworthy that for joints reinforced by shear reinforcements, although joint shear capacity would be improved and these sufficiently designed joints are capable of carrying the resulting principal tensile stresses, they can still lead to severe damage in the joint core due to principal compression stress,  $P_c$ . Accordingly, the shear strength is more likely to be governed by  $P_c$  which can be calculated approximately based on Mohr’s theory, using Eq. (14):

$$V_{jh} = \left( \sqrt{1 - \frac{f_v}{p_c}} \right) p_c b_j h_c \tag{14}$$

where  $p_c$  was considered equal to  $0.5 f'_c$  based on Priestley (1997).

### 4 Principal Tensile Stress: Joint Rotation Relation

In this section, the determination of the principal tensile stress—joint rotation relation for RC joints with various anchorages of beam bars in the joint core will be explained. In this study, according to the analytical studies conducted by Hassan (2011), Sharma et al. (2011) and Shayanfar et al. (2016), the effects of the bond-slip mechanism were indirectly considered in nonlinear analysis so that adding the joint rotation,  $\theta_j$ , as shown in Fig. 2, due to beam bar slip,  $\theta_{slip}$ , to joint shear deformation,  $\gamma_j$ , (Fig. 2) the rotation of the joint core can be determined ( $\theta_j = \gamma_j + \theta_{slip}$ ). In this paper, according to Shayanfar et al. (2016) with some modifications, for RC beam–column joints with various anchorages of beam longitudinal bars, principal tensile stress versus joint rotations can be calculated using the developed relations shown in Fig. 7.  $K_{deg}$  is the post-peak stiffness in principle tensile stress–joint rotation relation which for joints with 90°-hook bent in is 40 MPa/Rad. For joints with straight anchorage,  $K_{deg}^1$  and  $K_{deg}^2$  were considered equal to 35 and 12 MPa/Rad, respectively.

It should be noted that for joints with 90°-hook bent in the joint core, shear reinforcements do not have any effect on the strength of the first cracking in the joint core due to the fact that they cannot change the material characteristic of concrete. In other words, the effect of shear reinforcements in the joint core can be exposed after the first cracking. However, maximum joint strength can increase using shear reinforcement. Accordingly, in this study, this effect of stirrups was merely considered on maximum principal tensile stress. Although it might influence initial stiffness of RC joints (Liu 2006; Shayanfar et al. 2016), in the present work, to be conservative, this effect was ignored.

For other anchorage types of beam bars, as it was discussed, if adequate shear reinforcements were provided in the core of an RC joint, the failure mechanism would tend to be similar to the failure mechanism of RC joints with 90°-hook bent in the joint core. Therefore, to determine governed failure mechanism in an RC joint with an anchorage type except for joints with 90°-hooks bent in, the joint strength can be calculated comparing  $p_{t,max}$  in joints with 90°-hooks bent in without considering the effect of shear reinforcement ( $S_j = 0$  in Eq. 10) to one

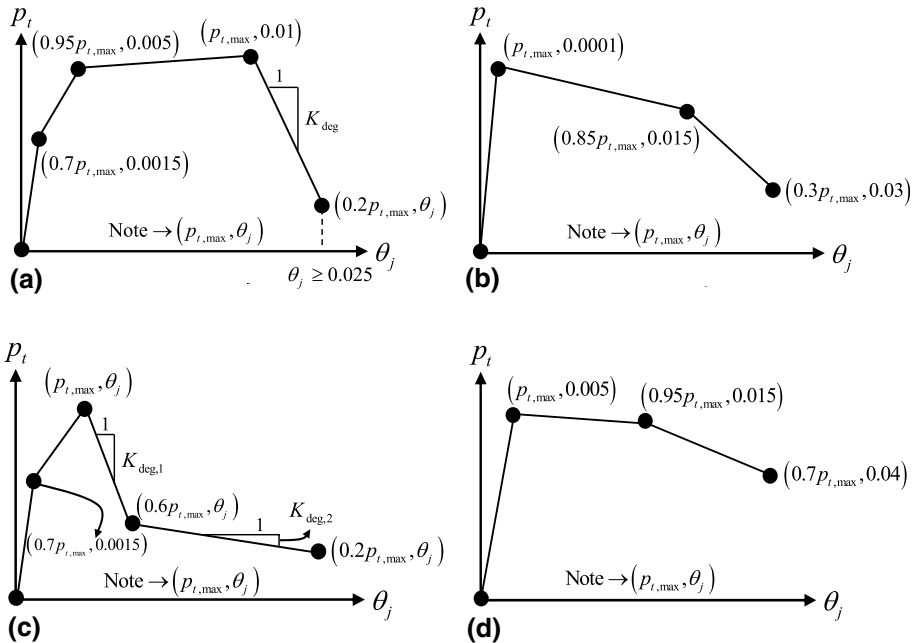


**Fig. 7** Principal tensile stress versus joint rotation. **a** beam bars bent in the joint core, **b** end-hook anchorage, **c** straight anchorage, **d** beam bars bent away from the joint core

corresponding to joint anchorage type with considering the shear reinforcement effect on joint capacity. Accordingly, at least two values can determine the joint failure mechanism and subsequently, the type of principal tensile stress versus joint rotation in the joint core.

In other words, for an RC joint with an anchorage type except for joints with 90°-hooks bent in, if adequate shear reinforcements were considered in the core of an RC joint, the proposed principal tensile stress versus joint rotation in Fig. 7a could be used and otherwise, the relation recommended corresponding to joint anchorage type could be followed.

## 5 Flexural and shear behavior in beam/column

In this section, the calculation of the rotational spring characteristics in seismically prone areas will be addressed. To determine flexural characteristics in terms of flexural moment versus rotation relation, the moment–curvature analysis can be useful. After which, the rotation of the beam/column elements corresponding to the curvature obtained from the analysis can be calculated through the plastic hinge approach suggested by Priestley et al. (1996). On the other hand, inadequate shear capacity in RC beam/columns is one of the most important shortages of RC structures probably making these members completely vulnerable against seismic loading (Lynn 2001; Sezen 2002; Elwood 2002). In this study, to calculate shear as well as flexural behavior of an RC beam/columns, the fiber model developed by Shay-anfar and Akbarzadeh (2017) was followed. To calculate flexural characteristics, the effects of concrete confinement and buckling of longitudinal reinforcements were considered in the model of moment–curvature analysis along with another model for simulating the axial load

variation effect at the structural level. Likewise, the shear capacity as a function of the curvature ductility was assumed as the sum of shear strengths due to concrete and stirrup (Fig. 8).

$$V_n = \sum v(x)bt_s + \frac{A_s f_{yv} d}{s} \tag{15}$$

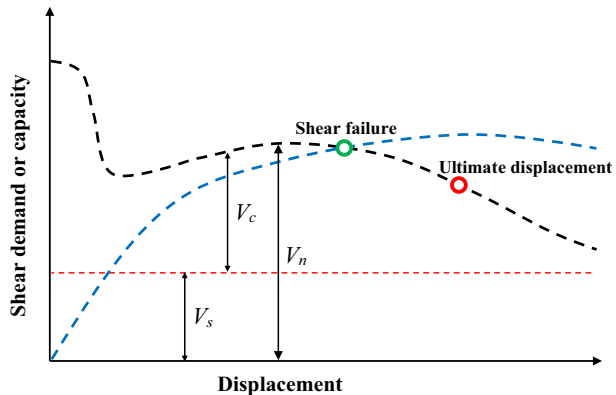
where  $t_s$ =the strip thickness in the cross section;  $b$ =the member width;  $A_s$ =the total stirrup area in the beam/column;  $s$ =the centre to centre spacing of the stirrup;  $f_{yv}$ =the yield stress of the stirrup;  $d$ =the effective depth of cross-section;  $v(x)$ =the concrete shear stress acting on an element of the compression regions of the cross section corresponding to the normal stress  $f_c(x)$  as well as tensile and compression strength of concrete as principle tensile and compression stresses based on Mohr’s theory. The further details of the model can be found in Shayanfar and Akbarzadeh (2017).

### 6 Validation of the proposed model with experiments

This section addresses the reliability of the proposed analytical model to carry out non-linear analysis on RC beam–column joints. The results obtained from nonlinear analyses were compared to experimental results. For each specimen, in order to appropriately assess the dominant role of the joint core in nonlinear analyses, two nonlinear analyses were performed, one taking into account the joint nonlinearities in nonlinear analyses and another assuming the joint core as rigid. To extensively verify the capability of the joint model, the results of the numerical analyses on RC joints in terms of the maximum principle tensile stress and the horizontal shear strength in the joint core were also compared to experimental results reported by other researchers (Appendix Table 2). It should be noted that nonlinear analyses were carried out via the commercial software SAP 2000 (2008). In Fig. 9, a flowchart was provided for obtaining the characteristics of diagonal axial springs of  $P_j - \Delta_j$  of the joint core. As can be seen, the diagonal axial spring characteristics can be easily obtained by converting the proposed principle tensile stress–joint rotation relation into axial load–axial displacement relation.

On the other hand, once beam/column moment–curvature relation was determined, flexural and shear capacities can be computed by the simple procedure to control shear mechanism as developed by Shayanfar and Akbarzadeh (2017).

**Fig. 8** Shear model developed by Shayanfar and Akbarzadeh (2017)



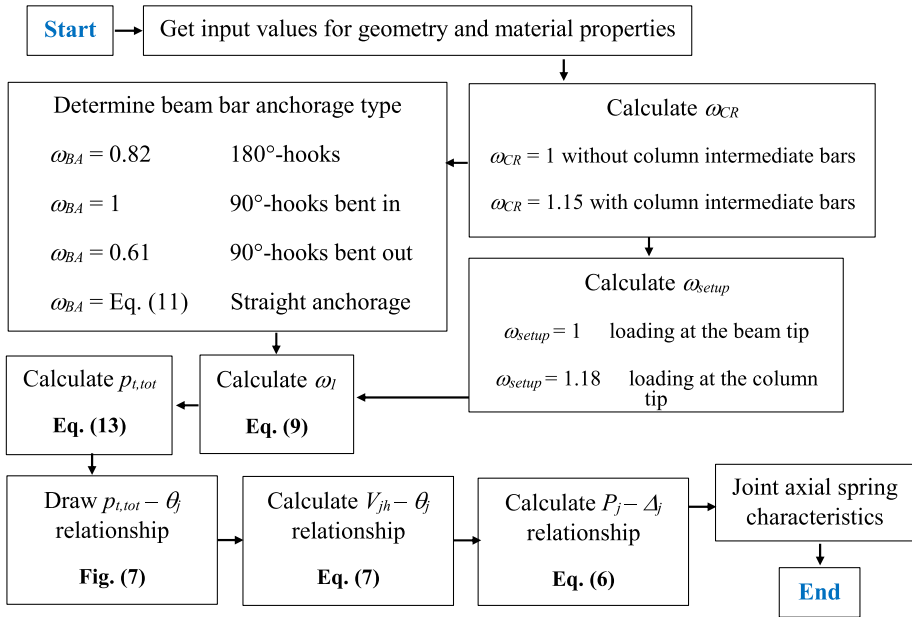


**Fig. 9** A flowchart for obtaining the characteristics of the diagonal axial springs

Wong (2005) conducted an experimental study on exterior RC beam–column joints with different beam bar anchorages and various joint shear reinforcements. The beam longitudinal bars were anchored as 90°-hooks. All specimens were designed without shear reinforcement in the joint core. In the specimens BS-OL and BS-LL, beam bar anchorage was considered 90°-hooks bent out and other ones were anchored as 90°-hooks bent in. In the specimens BS-L-V2 and BS-L-V4, column intermediate reinforcements was considered and other ones were designed with no column intermediate bars. Specimens BS-L-H1T10, BS-L-H2T10, BS-L-H2T8 and BS-L-H4T8 were reinforced by shear reinforcements and the others were with no shear reinforcements. Complete detailed of the tested specimens can be found from Wong (2005).

In Fig. 10, the responses obtained from the tests and the numerical analyses were compared. As can be observed, the close agreement between experimental and numerical results confirms that the proposed joint model is capable of simulating the response of the RC joints. Likewise, as it was expected, without modelling nonlinearities in the joint region, the higher ductility and strength than the results reported from the tests were estimated. For the specimens with 90°-hooks bent out, the assumption for the principle tensile stress–joint rotation relation seems to be correct according to the simulation results. For the specimens with the column intermediate bars, with the increase of 15% in the maximum value of principle tensile stress, the RC joint analyses led to the results with reasonable accurate. For the specimens with shear reinforcements, the model was capable of predicting the response of the RC joints with shear failure in the joint core.

It should be noted that load versus displacement responses of other test specimens were also compared with the simulations obtained from the numerical model in Fig. 11. Complete detailed of the tested specimens can be found from Table 1. As can be observed in the figure, the nonlinear analysis considering the joint core as rigid led to quite unsafe



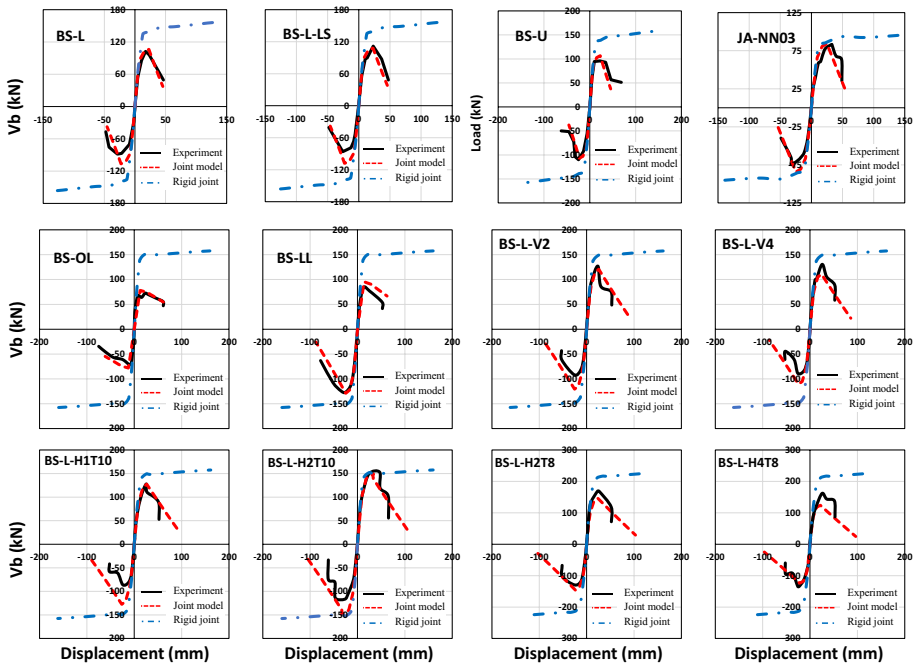


Fig. 10 Validation of the proposed numerical model against test results reported by Wong (2005)

estimation of the response, whereas using the developed beam–column joint model, the nonlinear analysis induced to results in close agreement with the experimental counterparts. It can be regarded as a further validation of the numerical joint model.

In the following, the capability of the developed beam–column joint model in estimating the maximum principle tensile stress and horizontal shear strength in the joint core will be addressed. For this, the proposed principle tensile stress and the corresponding shear strength were applied to the tested specimens as shown in Fig. 12 and Appendix Table 2. As can be observed, using the beam–column joint model, the mean of the ratio of the principle tensile stress and horizontal shear strength obtained-to-experimental was calculated equal to 0.99 and 0.98 with SD 0.27 and 0.18 along with a MAPE, 19.4% and 14.6%, respectively. Accordingly, it could be concluded that for RC joints with various beam bar anchorages, the developed beam–column joint model is able to present the uniform prediction of RC joint response with reasonable precision and a relatively low level of dispersion.

Figure 13 illustrates the variations of horizontal shear strength in the test specimen of Wong (2005) for a range of axial load index, joint shear reinforcement ratios, beam bar index and beam depth. The selected specimen was BS-L, which was not reinforced by shear reinforcement and was anchored as 90°-hooks bent in. no intermediate longitudinal bar was considered in the column ( $\omega_{CR}=0$ ). Complete detailed of the tested specimen can be found from Wong (2005). As can be observed in Fig. 13a, according to the proposed model [Eqs. (7) and (8)], joint horizontal shear strength enhanced increasing  $r_B$ . In Fig. 13b, c, the increase of joint shear reinforcement ratios and beam depth, the shear strength increased and decreased, respectively. A closer at the data reveals that increasing the level of axial load, the variations and effects of the mentioned factors on joint capacity significantly dropped. It should be noted that according to Eq. (7), for a constant value

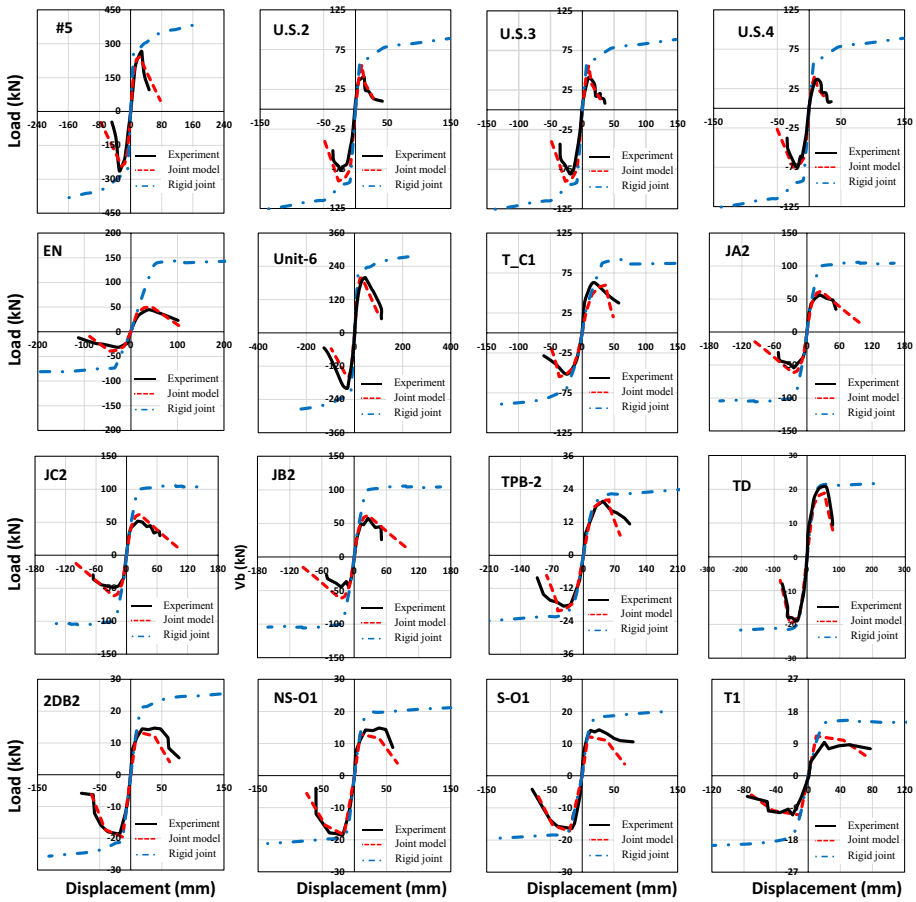


Fig. 11 Validation of the proposed numerical model against test results

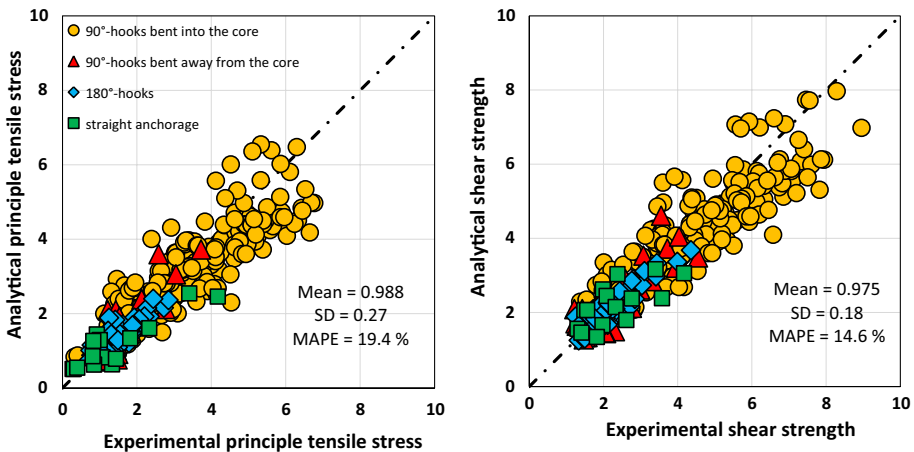
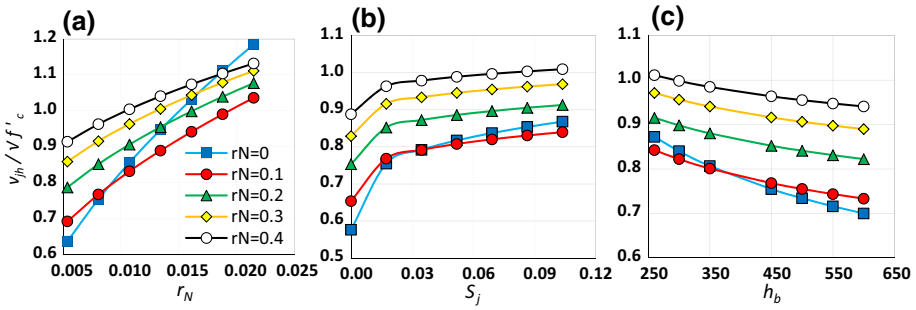


Fig. 12 Comparison of calculated and experimental joint principle tensile stress and shear strength



**Fig. 13** Variations of principle tensile stress in the test specimen of Wong (2005): **a** beam bar index; **b** joint shear reinforcement index; **c** beam depth

of principle tensile stress, axial load increases the joint shear capacity, while based on Eq. (10), axial load negatively influences it. Therefore, interaction between the effects of axial load on principle tensile stress and horizontal shear strength can cause a decrease in the effects of the influential factors. Accordingly, based on the results of the parametric study, the effectiveness of the influential factors of RC beam–column joints is noticeably a function of the level of the axial load applied on the column.

### 7 Conclusion

In the present paper, to account for nonlinearities in the joint core, based on theoretical formulations and experimental observations, a new simplified procedure was developed for numerically modelling RC beam–column joints. For this purpose, a joint model was proposed so that nonlinearities in the joint core were simulated by two diagonal axial springs. In the model, the effects of the main factors influencing the mechanical behavior of RC joints i.e. column intermediate bars, joint aspect ratio, joint shear reinforcements, type of beam bar anchorage, etc. were considered. According to the principal stress approach, a more refined calibration of principle tensile stress versus joint rotation relation was developed to calculate characteristics of these springs. To evaluate the reliability and capability of the developed numerical model, results obtained from nonlinear analyses, considering the joint core behavior, were compared to the ones reported from existing experimental results. It proved that the joint model is prone to predicting the response of RC beam–column joints with reasonable accuracy. According to this study, assuming the joint core to behave as a rigid, even for joints reinforced by shear reinforcements might bring about unsafe and non-conservative predictions in terms of both strength and ductility capacities. On the other hand, based on the parametric study, it was concluded that the effectiveness of the influential factors of RC beam–column joints is noticeably a function of the level of the axial load applied on the column. Ultimately, the simplified numerical model could provide a practical but reasonably accurate procedure to model inelastic behavior of the joint core in nonlinear analyses.

### Appendix

See Table 2.

**Table 2** Database of experimental tests on exterior RC beam–column joints

Test ID	Type	$\alpha_{semp}$	CIR <sup>e</sup>	$f'_c$ (MPa)	$\frac{h_c}{b_c}$	$\alpha$	$r_B$	$r_N$	$\rho_{sj}$	$P_{r,tot}^{exp}$	$P_{r,tot}$	$\frac{exp}{ana}$	$v_{jh}^{exp}$	$v_{jh}^{ana}$	$\frac{exp}{ana}$	
Clyde et al. (2000)																
#2	A <sup>a</sup>	1.00	1	46	1.33	0.89	0.21	0.11	0.00	0.77	0.60	0.78	1.08	0.89	0.83	
#4	A	1.00	1	41	1.33	0.89	0.23	0.24	0.00	0.62	0.49	0.79	1.16	1.00	0.86	
#5	A	1.00	1	37	1.33	0.89	0.26	0.28	0.00	0.55	0.47	0.85	1.11	1.01	0.91	
#6	A	1.00	1	41	1.33	0.89	0.23	0.10	0.00	0.81	0.61	0.76	1.09	0.88	0.81	
Kang et al. (2010)																
JK	A	1.00	1	29	1.20	1.20	0.07	0.00	0.04	0.54	0.64	1.17	0.54	0.64	1.17	
Campione et al. (2016)																
C1 specimen																
Sasmal (2009)																
SP-1	A	1.00	0	30	1.33	1.33	0.11	0.11	0.02	0.50	0.46	0.90	0.75	0.70	0.93	
SP-3	A	1.00	1	30	1.33	1.33	0.27	0.11	0.03	0.82	0.75	0.91	1.08	1.01	0.93	
SP-3	A	1.00	1	30	1.33	1.33	0.18	0.11	0.03	0.84	0.63	0.75	1.11	0.89	0.80	
SP-4	A	1.00	1	30	1.33	1.33	0.22	0.11	0.06	0.78	0.71	0.91	1.04	0.97	0.93	
SP-4	A	1.00	1	30	1.33	1.33	0.14	0.11	0.06	0.59	0.60	1.01	0.85	0.85	1.00	
SP-5	A	1.00	1	30	1.33	1.33	0.27	0.11	0.09	1.00	0.80	0.81	1.26	1.06	0.84	
SP-5	A	1.00	1	30	1.33	1.33	0.18	0.11	0.09	0.98	0.68	0.69	1.25	0.94	0.75	
SP-6	A	1.00	1	30	1.33	1.33	0.22	0.11	0.05	0.87	0.71	0.81	1.13	0.96	0.85	
SP-6	A	1.00	1	30	1.33	1.33	0.14	0.11	0.05	0.70	0.60	0.85	0.96	0.85	0.88	
Hamil (2000)																
C4ALNO	A	1.00	0	42	1.91	1.40	0.12	0.05	0.00	0.65	0.49	0.76	0.82	0.66	0.80	
C4ALN1	A	1.00	0	46	1.91	1.40	0.11	0.05	0.02	0.83	0.63	0.76	1.00	0.80	0.80	
C4ALN3	A	1.00	0	42	1.91	1.40	0.12	0.05	0.06	0.92	0.68	0.74	1.10	0.86	0.78	
C4ALN5	A	1.00	0	50	1.91	1.40	0.10	0.04	0.08	0.95	0.70	0.73	1.12	0.86	0.77	
C6LNO	A	1.00	0	51	1.91	1.40	0.10	0.04	0.00	0.52	0.49	0.95	0.67	0.64	0.96	
C6LNI	A	1.00	0	51	1.91	1.40	0.10	0.04	0.02	0.54	0.62	1.17	0.69	0.78	1.13	
C6LN3	A	1.00	0	49	1.91	1.40	0.10	0.05	0.05	0.66	0.67	1.02	0.83	0.84	1.01	

Table 2 (continued)

Test ID	Type	$\alpha_{setup}$	CIR <sup>e</sup>	$f'_c$ (MPa)	$\frac{h_c}{b_c}$	$\alpha$	$r_B$	$r_N$	$\rho_{s,j}$	$P_{r,tot}^{exp}$	$P_{r,tot}$	$\frac{exp}{ana}$	$v_{jh}^{exp}$	$v_{jh}^{ana}$	$\frac{exp}{ana}$
C6LN5	A	1.00	0	37	1.91	1.40	0.13	0.06	0.11	0.93	0.72	0.77	1.12	0.90	0.80
C6LHO	A	1.00	0	101	1.91	1.40	0.05	0.04	0.00	0.51	0.45	0.89	0.72	0.66	0.92
C6LH1	A	1.00	0	102	1.91	1.40	0.05	0.04	0.01	0.53	0.55	1.05	0.74	0.77	1.04
C6LH3	A	1.00	0	97	1.91	1.40	0.05	0.05	0.03	0.62	0.59	0.95	0.84	0.81	0.96
C4ALN1T	A	1.00	0	40	1.91	1.40	0.12	0.06	0.02	0.80	0.63	0.79	0.98	0.81	0.83
C6LN1B	A	1.00	0	39	1.91	1.40	0.13	0.06	0.02	0.54	0.63	1.16	0.72	0.81	1.13
C6LN1T	A	1.00	0	40	1.91	1.40	0.12	0.06	0.02	0.68	0.63	0.93	0.86	0.81	0.95
C6LN1A	A	1.00	0	49	1.91	1.40	0.10	0.05	0.02	0.62	0.63	1.00	0.79	0.79	1.00
C6LN2A	A	1.00	0	51	1.91	1.40	0.10	0.04	0.03	0.70	0.65	0.94	0.86	0.81	0.95
C6LN2B	A	1.00	0	51	1.91	1.40	0.10	0.04	0.03	0.82	0.65	0.79	0.99	0.81	0.82
C6LN3A	A	1.00	0	46	1.91	1.40	0.11	0.05	0.05	0.74	0.68	0.91	0.91	0.84	0.93
C6LN3B	A	1.00	0	52	1.91	1.40	0.09	0.04	0.05	0.89	0.67	0.75	1.05	0.83	0.79
C6LN3C	A	1.00	0	48	1.91	1.40	0.10	0.05	0.05	0.83	0.67	0.81	1.00	0.84	0.84
C7LNO	A	1.00	0	38	2.73	2.00	0.09	0.06	0.00	0.59	0.46	0.78	0.77	0.63	0.82
C7LN1	A	1.00	0	38	2.73	2.00	0.09	0.06	0.02	0.68	0.58	0.86	0.86	0.76	0.88
C7LN3	A	1.00	0	40	2.73	2.00	0.09	0.06	0.05	0.82	0.62	0.76	1.00	0.80	0.80
C7LN5	A	1.00	0	40	2.73	2.00	0.09	0.06	0.08	0.95	0.65	0.68	1.14	0.82	0.72
C9LNO	A	1.00	0	41	2.73	2.00	0.08	0.05	0.00	0.52	0.46	0.88	0.70	0.63	0.90
C9LN1	A	1.00	0	38	2.73	2.00	0.09	0.06	0.02	0.54	0.58	1.08	0.71	0.76	1.06
C9LN3	A	1.00	0	37	2.73	2.00	0.09	0.06	0.05	0.65	0.62	0.96	0.83	0.81	0.97
C9LN5	A	1.00	0	35	2.73	2.00	0.10	0.06	0.09	0.84	0.65	0.78	1.03	0.84	0.81
C6LN1(r)	A	1.00	0	49	1.91	1.40	0.10	0.09	0.02	0.51	0.56	1.11	0.80	0.85	1.07
C6LN1AE	A	1.00	0	44	1.91	1.40	0.11	0.05	0.02	0.70	0.63	0.90	0.87	0.80	0.92
C4ALN1CY	A	1.00	0	44	1.91	1.40	0.11	0.05	0.02	1.00	0.63	0.63	1.18	0.80	0.68
C4ALN3CY	A	1.00	0	44	1.91	1.40	0.11	0.05	0.06	0.95	0.68	0.71	1.13	0.85	0.75

**Table 2** (continued)

Test ID	Type	$\alpha_{setup}$	CIR <sup>e</sup>	$f'_c$ (MPa)	$\frac{h_c}{b_c}$	$\alpha$	$r_B$	$r_N$	$\rho_{s,j}$	$P_{r,tot}^{exp}$	$P_{r,tot}^{ana}$	$\frac{exp}{ana}$	$v_{jh}^{exp}$	$v_{jh}^{ana}$	$\frac{exp}{ana}$	
C6LN1CY	A	1.00	0	45	1.91	1.40	0.11	0.05	0.02	0.71	0.63	0.89	0.88	0.80	0.91	
C6LN3CY	A	1.00	0	42	1.91	1.40	0.12	0.05	0.06	0.76	0.68	0.90	0.94	0.86	0.92	
C6LN5CY	A	1.00	0	45	1.91	1.40	0.11	0.05	0.09	0.88	0.71	0.80	1.06	0.88	0.83	
C6LN7CY	A	1.00	0	47	1.91	1.40	0.10	0.05	0.12	0.97	0.72	0.74	1.15	0.89	0.78	
C6LN3CYE	A	1.00	0	44	1.91	1.40	0.11	0.05	0.06	0.82	0.68	0.82	1.00	0.85	0.85	
Realfonzo et al. (2014)																
J-05	A	1.00	0	15	1.33	1.33	0.38	0.23	0.00	0.45	0.39	0.87	0.77	0.70	0.91	
J-01	A	1.00	0	16	1.33	1.33	0.26	0.20	0.00	0.39	0.37	0.95	0.69	0.66	0.96	
Murty et al. (2003)																
P1	A	1.00	1	27	2.00	1.60	0.12	0.00	0.00	0.77	0.63	0.83	0.77	0.63	0.83	
P2	A	1.00	1	26	2.00	1.60	0.12	0.00	0.03	0.97	0.85	0.88	0.97	0.85	0.88	
P3	A	1.00	1	27	2.00	1.60	0.12	0.00	0.02	0.84	0.84	1.01	0.84	0.84	1.01	
Q1	A	1.00	1	26	2.00	1.60	0.13	0.00	0.00	0.72	0.64	0.88	0.72	0.64	0.88	
Q2	A	1.00	1	27	2.00	1.60	0.12	0.00	0.02	0.98	0.84	0.86	0.98	0.84	0.86	
Q3	A	1.00	1	27	2.00	1.60	0.12	0.00	0.02	0.95	0.85	0.89	0.95	0.85	0.89	
R1	A	1.00	1	30	2.00	1.60	0.11	0.00	0.00	0.74	0.63	0.85	0.74	0.63	0.85	
R2	A	1.00	1	27	2.00	1.60	0.12	0.00	0.02	1.03	0.84	0.82	1.03	0.84	0.82	
R3	A	1.00	1	27	2.00	1.60	0.12	0.00	0.02	0.98	0.84	0.86	0.98	0.84	0.86	
S1	A	1.00	1	28	2.00	1.60	0.12	0.00	0.00	0.72	0.63	0.87	0.72	0.63	0.87	
S2	A	1.00	1	27	2.00	1.60	0.12	0.00	0.03	0.98	0.85	0.86	0.98	0.85	0.86	
S3	A	1.00	1	30	2.00	1.60	0.11	0.00	0.02	0.84	0.83	0.98	0.84	0.83	0.98	
Chun et al. (2007)																
JC-2	A	1.00	1	60	1.43	1.00	0.12	0.03	0.01	0.58	0.77	1.33	0.72	0.91	1.27	
JC-11	A	1.00	1	33	1.12	0.97	0.19	0.00	0.03	0.72	0.97	1.35	0.72	0.97	1.35	

**Table 2** (continued)

Test ID	Type	$\alpha_{setup}$	CIR <sup>e</sup>	$f'_c$ (MPa)	$\frac{h_c}{b_c}$	$\alpha$	$r_B$	$r_N$	$\rho_{s,j}$	$P_{r,tot}^{exp}$	$P_{r,tot}$	$\frac{exp}{ana}$	$V_{jh}^{exp}$	$V_{jh}^{ana}$	$\frac{exp}{ana}$	
<b>Hwang et al. (2005)</b>																
OT0	A	1.00	1	67	1.41	1.07	0.09	0.02	0.00	0.59	0.61	1.02	0.67	0.68	1.02	
1B8	A	1.00	1	62	1.41	1.07	0.10	0.02	0.03	0.80	0.82	1.03	0.88	0.90	1.02	
3T3	A	1.00	1	69	1.41	1.07	0.09	0.02	0.01	0.68	0.77	1.14	0.75	0.84	1.12	
2T4	A	1.00	1	71	1.41	1.07	0.09	0.02	0.02	0.63	0.78	1.23	0.70	0.85	1.20	
1T44	A	1.00	1	73	1.41	1.07	0.09	0.02	0.01	0.60	0.75	1.24	0.67	0.82	1.22	
<b>Ehsani et al. (1987)</b>																
3	A	1.00	1	65	1.69	1.46	0.08	0.07	0.04	0.58	0.66	1.13	0.82	0.90	1.10	
4	A	1.00	1	67	1.69	1.46	0.09	0.05	0.03	0.72	0.73	1.03	0.92	0.94	1.02	
5	A	1.00	1	44	1.69	1.46	0.11	0.06	0.05	0.83	0.73	0.88	1.01	0.91	0.90	
<b>Pantelides et al. (2002)</b>																
1	A	1.00	0	33	1.00	1.00	0.22	0.10	0.00	0.64	0.45	0.70	0.88	0.68	0.77	
2	A	1.00	0	30	1.00	1.00	0.24	0.27	0.00	0.48	0.36	0.73	0.98	0.81	0.83	
3	A	1.00	0	34	1.00	1.00	0.21	0.10	0.00	0.67	0.45	0.67	0.91	0.68	0.74	
4	A	1.00	0	32	1.00	1.00	0.23	0.27	0.00	0.55	0.36	0.65	1.07	0.82	0.76	
5	A	1.00	0	32	1.00	1.00	0.23	0.10	0.00	0.74	0.45	0.61	0.98	0.67	0.69	
6	A	1.00	0	31	1.00	1.00	0.23	0.26	0.00	0.52	0.36	0.70	1.01	0.81	0.80	
<b>Hadi and Tran (2016)</b>																
T0	A	1.00	0	41	1.50	1.50	0.10	0.00	0.00	0.56	0.53	0.95	0.56	0.53	0.95	
<b>Wong (2005)</b>																
BS-L-450	A	1.00	0	31	1.73	1.50	0.14	0.15	0.00	0.36	0.39	1.09	0.67	0.71	1.05	
BS-L-V2	A	1.00	1	33	1.73	1.50	0.13	0.15	0.00	0.48	0.45	0.93	0.82	0.78	0.95	
BS-L-V4	A	1.00	1	28	1.73	1.50	0.15	0.15	0.00	0.57	0.45	0.80	0.90	0.77	0.86	
BS-L-H1T10	A	1.00	0	33	1.73	1.50	0.13	0.15	0.02	0.46	0.48	1.04	0.80	0.82	1.03	
BS-L-H2T10	A	1.00	0	42	1.73	1.50	0.10	0.15	0.02	0.50	0.48	0.96	0.87	0.85	0.97	

**Table 2** (continued)

Test ID	Type	$\alpha_{setup}$	CIR <sup>e</sup>	$f'_c$ (MPa)	$\frac{h_c}{h_b}$	$\alpha$	$r_B$	$r_N$	$\rho_{s,j}$	$P_{r,tot}^{exp}$	$P_{r,tot}^{ana}$	$\frac{exp}{ana}$	$v_{jh}^{exp}$	$v_{jh}^{ana}$	$\frac{exp}{ana}$
BS-L-600	A	1.00	0	36	2.31	2.00	0.09	0.15	0.00	0.25	0.37	1.46	0.56	0.70	1.26
BS-L-H2T8	A	1.00	0	42	1.73	1.50	0.10	0.15	0.02	0.59	0.47	0.79	0.98	0.84	0.86
BS-L-H4T8	A	1.00	0	30	1.73	1.50	0.14	0.15	0.04	0.75	0.51	0.68	1.10	0.84	0.76
BS-L-L	A	1.00	0	42	1.73	1.50	0.10	0.15	0.00	0.37	0.38	1.02	0.73	0.74	1.01
BS-U	A	1.00	0	31	1.73	1.50	0.14	0.15	0.00	0.41	0.39	0.97	0.73	0.71	0.98
BS-L-LS	A	1.00	0	32	1.73	1.50	0.13	0.15	0.00	0.40	0.39	0.97	0.72	0.71	0.98
JA-NN15	A	1.00	0	46	1.54	1.33	0.07	0.15	0.02	0.22	0.43	2.00	0.53	0.81	1.53
JB-NN03	A	1.00	0	47	1.15	1.00	0.10	0.03	0.00	0.41	0.45	1.10	0.51	0.55	1.08
JA-NY03	A	1.00	0	35	1.54	1.33	0.10	0.03	0.03	0.48	0.57	1.18	0.57	0.66	1.16
JA-NY15	A	1.00	0	39	1.54	1.33	0.09	0.15	0.03	0.27	0.44	1.65	0.58	0.80	1.37
JA-NN03	A	1.00	0	45	1.54	1.33	0.08	0.03	0.00	0.41	0.43	1.04	0.51	0.53	1.03
Le-Trung et al. (2010)															
NS	A	1.18	0	37	1.49	1.20	0.10	0.00	0.00	0.76	0.45	0.60	0.64	0.45	0.71
Antonopoulos and Triantafyllou (2003)															
C1	A	1.00	0	16	1.50	1.50	0.29	0.07	0.00	0.44	0.46	1.05	0.57	0.59	1.04
C2	A	1.00	0	19	1.50	1.50	0.24	0.06	0.00	0.40	0.47	1.18	0.51	0.58	1.14
T-C	A	1.00	0	20	1.50	1.50	0.23	0.06	0.00	0.47	0.47	1.00	0.58	0.58	1.00
S-C	A	1.00	0	15	1.50	1.50	0.29	0.07	0.02	0.48	0.60	1.25	0.61	0.73	1.21
Ghobarah and Said (2001)															
TI	A	1.00	1	31	1.60	1.00	0.16	0.19	0.00	0.53	0.46	0.87	0.93	0.84	0.91
Garcia et al. (2013)															
JAE2	A	1.00	0	32	1.54	1.54	0.13	0.07	0.00	0.38	0.43	1.14	0.54	0.59	1.11
JB2	A	1.00	0	31	1.54	1.54	0.14	0.07	0.00	0.39	0.43	1.11	0.55	0.60	1.08
JC2	A	1.00	0	32	1.54	1.54	0.13	0.07	0.00	0.35	0.43	1.22	0.51	0.59	1.16



**Table 2** (continued)

Test ID	Type	$\alpha_{seisup}$	CIR <sup>e</sup>	$f'_c$ (MPa)	$\frac{h_c}{b_c}$	$\alpha$	$r_B$	$r_N$	$\rho_{sij}$	$P_{r,tot}^{exp}$	$P_{r,tot}^{ana}$	$\frac{exp}{ana}$	$V_{jh}^{exp}$	$V_{jh}^{ana}$	$\frac{exp}{ana}$
El-Amoury (2003)															
T-S1	A	1.00	1	31	1.60	1.00	0.18	0.19	0.00	0.54	0.48	0.88	0.94	0.86	0.92
Ha et al. (2013)															
LBCJC	A	1.18	1	27	1.33	1.00	0.22	0.15	0.00	0.45	0.42	0.93	0.70	0.74	1.06
Shafaei et al. (2014)															
J2	A	1.00	1	23	1.14	1.00	0.22	0.15	0.00	0.42	0.46	1.09	0.71	0.75	1.06
J2	A	1.00	1	23	1.14	1.00	0.18	0.15	0.00	0.33	0.44	1.32	0.60	0.73	1.21
J3	A	1.00	1	25	1.14	1.00	0.21	0.14	0.00	0.49	0.46	0.94	0.78	0.75	0.96
Dhake et al. (2015)															
J2	A	1.00	0	30	1.20	0.90	0.15	0.11	0.07	0.54	0.55	1.01	0.79	0.80	1.01
Alva et al. (2007)															
LVP2	A	1.00	1	44	2.00	1.33	0.14	0.15	0.03	0.94	0.66	0.71	1.35	1.05	0.78
LVP3	A	1.00	1	24	2.00	1.33	0.25	0.15	0.10	0.95	0.79	0.83	1.26	1.09	0.87
LVP4	A	1.00	1	25	2.00	1.33	0.24	0.15	0.05	0.80	0.74	0.92	1.12	1.05	0.94
LVP5	A	1.00	1	26	2.00	1.33	0.23	0.15	0.09	0.94	0.77	0.83	1.26	1.09	0.86
Shrestha et al. (2009)															
UC1	A	1.00	0	26	1.50	1.50	0.28	0.08	0.00	0.46	0.51	1.13	0.62	0.68	1.10
Melo et al. (2012)															
TPA-1	A	1.18	0	24	1.60	1.60	0.06	0.13	0.00	0.29	0.26	0.89	0.47	0.48	1.03
TPA-2	A	1.18	0	26	1.60	1.60	0.05	0.12	0.00	0.30	0.26	0.86	0.47	0.48	1.01
TPB-1	A	1.18	0	16	1.60	1.60	0.09	0.20	0.00	0.35	0.25	0.71	0.57	0.51	0.89
TPB-2	A	1.18	0	27	1.60	1.60	0.05	0.12	0.00	0.29	0.26	0.88	0.46	0.48	1.03
TP	A	1.18	0	22	1.60	1.60	0.07	0.15	0.00	0.36	0.26	0.73	0.55	0.50	0.91
Hertanto (2005)															
TDD-2	A	1.18	0	25	1.50	1.30	0.11	0.09	0.01	0.49	0.39	0.79	0.61	0.58	0.95

**Table 2** (continued)

Test ID	Type	$\alpha_{semap}$	CIR <sup>e</sup>	$f'_c$ (MPa)	$\frac{h_c}{b_c}$	$\alpha$	$r_B$	$r_N$	$\rho_{sj}$	$P_{r,tot}^{exp}$	$P_{r,tot}$	$\frac{exp}{ana}$	$v_{jh}^{exp}$	$v_{jh}^{ana}$	$\frac{exp}{ana}$	
TDD-2	A	1.18	0	25	1.50	1.30	0.08	0.03	0.01	0.41	0.38	0.93	0.43	0.46	1.08	
Santarsiero and Masi (2015)																
SJ	A	1.18	0	22	1.67	1.67	0.09	0.15	0.08	0.43	0.35	0.81	0.62	0.61	0.97	
SJ	A	1.18	0	22	1.67	1.67	0.08	0.15	0.08	0.37	0.33	0.90	0.57	0.59	1.04	
Biddah (1997)																
J4	A	1.18	1	24	1.00	1.20	0.07	0.07	0.00	0.37	0.32	0.84	0.45	0.45	1.00	
Kaku and Asakusa (1991)																
4D16.H6+01	A	1.18	0	42	1.38	1.00	0.13	0.00	0.02	0.98	0.70	0.71	0.83	0.70	0.83	
4D16.H3+18	A	1.18	0	31	1.38	1.00	0.18	0.17	0.01	0.76	0.42	0.55	1.06	0.80	0.75	
4D16.H3+09	A	1.18	0	37	1.38	1.00	0.15	0.09	0.01	0.76	0.47	0.62	0.90	0.72	0.80	
4D16.H3+00	A	1.18	0	40	1.38	1.00	0.14	0.00	0.01	0.96	0.65	0.67	0.82	0.65	0.79	
4D10.8D10.H6+01	A	1.18	1	41	1.38	1.00	0.14	0.00	0.02	1.08	0.81	0.74	0.92	0.81	0.88	
4D10.8D10.H3+09	A	1.18	1	42	1.38	1.00	0.13	0.08	0.01	0.75	0.54	0.72	0.89	0.78	0.88	
4D10.8D10.H3+01	A	1.18	1	35	1.38	1.00	0.16	0.00	0.01	1.03	0.77	0.75	0.87	0.77	0.88	
4D10.8D10.H6-05	A	1.18	1	46	1.38	1.00	0.12	-0.04	0.02	1.13	0.78	0.69	0.76	0.58	0.76	
4D13.8D06.H3+09	A	1.18	1	41	1.38	1.00	0.14	0.08	0.01	0.74	0.54	0.73	0.88	0.78	0.90	
4D13.4D10.H3+09	A	1.18	1	40	1.38	1.00	0.14	0.08	0.01	0.77	0.54	0.70	0.91	0.79	0.87	
4D10.8D06.H6+01	A	1.18	1	40	1.38	1.00	0.14	0.00	0.02	0.82	0.81	0.99	0.69	0.81	1.16	
Ha et al. (2013)																
LBCJC	A	1.00	1	27	1.33	1.00	0.22	0.15	0.00	0.39	0.50	1.29	0.70	0.83	1.18	
De Risi et al. (2016a, b)																
1	A	1.00	0	29	1.67	1.67	0.14	0.10	0.00	0.32	0.41	1.27	0.53	0.63	1.18	
2	A	1.00	0	29	1.67	1.67	0.05	0.10	0.00	0.23	0.31	1.37	0.42	0.52	1.24	
Yurdakul and Avsar (2016)																
EJ-R	A	1.18	0	8	2.00	1.00	0.37	0.00	0.00	0.83	0.56	0.68	0.70	0.56	0.80	

**Table 2** (continued)

Test ID	Type	$\alpha_{seup}$	CIR <sup>e</sup>	$f'_c$ (MPa)	$\frac{h_c}{b_c}$	$\alpha$	$r_B$	$r_N$	$\rho_{s,j}$	$P_{r,tot}^{exp}$	$P_{r,tot}^{ana}$	$\frac{exp}{ana}$	$V_{jh}^{exp}$	$V_{jh}^{ana}$	$\frac{exp}{ana}$	
<b>Tsonos and Papanikolaou (2003)</b>																
F1	A	1.18	1	20	1.50	1.50	0.20	0.25	0.00	0.71	0.33	0.47	1.02	0.70	0.69	
F2	A	1.18	1	31	1.50	1.50	0.11	0.16	0.00	0.48	0.34	0.72	0.72	0.65	0.90	
L1	A	1.18	1	34	1.50	1.50	0.16	0.15	0.00	0.53	0.39	0.75	0.76	0.70	0.92	
<b>Tsonos (2007)</b>																
G1	A	1.18	1	22	1.50	1.50	0.23	0.23	0.04	0.66	0.46	0.70	0.96	0.84	0.88	
E1	A	1.18	1	22	1.50	1.50	0.23	0.23	0.10	1.14	0.49	0.43	1.40	0.87	0.62	
<b>Tsonos et al. (1992)</b>																
S1	A	1.00	1	37	1.50	1.50	0.15	0.11	0.06	0.39	0.66	1.67	0.64	0.93	1.45	
S2	A	1.00	1	26	1.50	1.50	0.11	0.15	0.08	0.36	0.52	1.45	0.64	0.83	1.29	
S6	A	1.00	1	24	1.50	1.50	0.22	0.17	0.09	0.72	0.64	0.89	1.05	0.97	0.92	
S*6	A	1.00	0	29	1.50	1.50	0.19	0.14	0.07	0.84	0.57	0.68	1.15	0.86	0.75	
F2	A	1.00	0	24	1.50	1.50	0.22	0.17	0.09	0.56	0.56	0.99	0.88	0.88	0.99	
P1	A	1.00	0	33	1.50	1.50	0.16	0.12	0.06	0.59	0.57	0.96	0.87	0.85	0.97	
<b>Tsonos (2002)</b>																
O1	A	1.00	0	16	1.50	1.50	0.31	0.25	0.00	0.45	0.37	0.81	0.81	0.71	0.88	
O2	A	1.00	0	16	1.50	1.50	0.31	0.25	0.00	0.48	0.37	0.77	0.84	0.71	0.84	
<b>Tsonos (2014)</b>																
O3	A	1.00	0	9	1.50	1.50	0.55	0.44	0.00	0.50	0.31	0.62	0.95	0.71	0.75	
<b>Parvin et al. (2010)</b>																
U.S.2	A	1.18	0	25	1.67	1.67	0.11	0.31	0.00	0.22	0.25	1.13	0.57	0.67	1.17	
U.S.3	A	1.18	0	25	1.67	1.67	0.11	0.31	0.00	0.23	0.25	1.07	0.59	0.67	1.14	
U.S.4	A	1.18	0	25	1.67	1.67	0.11	0.16	0.00	0.34	0.29	0.85	0.56	0.56	1.00	
<b>Karayannis and Sirkelis(2008)</b>																
AI	A	1.00	0	36	1.50	1.50	0.04	0.05	0.00	0.22	0.33	1.53	0.33	0.45	1.37	

**Table 2** (continued)

Test ID	Type	$\alpha_{setup}$	CIR <sup>e</sup>	$f'_c$ (MPa)	$\frac{h_c}{b_c}$	$\alpha$	$r_B$	$r_N$	$\rho_{s,j}$	$P_{r,tot}^{exp}$	$P_{r,tot}$	$\frac{exp}{ana}$	$v_{jh}^{exp}$	$v_{jh}^{ana}$	$\frac{exp}{ana}$	
A2	A	1.00	0	36	1.50	1.50	0.04	0.05	0.00	0.19	0.33	1.77	0.30	0.45	1.52	
B1	A	1.00	0	36	1.50	1.50	0.04	0.05	0.09	0.22	0.43	1.96	0.33	0.55	1.66	
Karayannis et al. (2008)																
A0	A	1.00	0	32	1.50	1.50	0.05	0.06	0.00	0.23	0.33	1.44	0.35	0.46	1.31	
A1	A	1.00	0	32	1.50	1.50	0.05	0.06	0.03	0.25	0.40	1.62	0.37	0.53	1.43	
A2	A	1.00	0	32	1.50	1.50	0.05	0.06	0.05	0.28	0.42	1.51	0.40	0.55	1.37	
A3	A	1.00	0	32	1.50	1.50	0.05	0.06	0.08	0.27	0.43	1.58	0.40	0.56	1.42	
B0	A	1.00	0	32	1.50	1.00	0.14	0.04	0.00	0.48	0.50	1.02	0.58	0.59	1.02	
B1	A	1.00	0	32	1.50	1.00	0.14	0.04	0.02	0.54	0.65	1.20	0.63	0.74	1.17	
C0	A	1.00	1	32	1.50	1.00	0.14	0.04	0.00	0.52	0.56	1.07	0.62	0.66	1.06	
C2	A	1.00	1	32	1.50	1.00	0.14	0.04	0.04	0.52	0.77	1.47	0.61	0.86	1.40	
Chalioris et al. (2008)																
JA-0	A	1.00	1	34	1.50	1.00	0.13	0.03	0.00	0.52	0.56	1.08	0.61	0.65	1.07	
JCa-0	A	1.00	0	21	2.00	1.00	0.18	0.10	0.00	0.51	0.46	0.91	0.70	0.65	0.93	
JCb-0	A	1.00	0	23	2.00	1.00	0.24	0.10	0.00	0.65	0.53	0.81	0.86	0.73	0.85	
JB-0	A	1.00	0	32	1.50	1.00	0.14	0.04	0.00	0.48	0.50	1.04	0.57	0.59	1.03	
JB-s1	A	1.00	0	32	1.50	1.00	0.14	0.04	0.02	0.54	0.65	1.19	0.64	0.74	1.16	
JCa-s1	A	1.00	0	21	2.00	1.00	0.18	0.10	0.08	0.57	0.65	1.15	0.76	0.85	1.12	
JCa-s2	A	1.00	0	21	2.00	1.00	0.18	0.10	0.16	0.57	0.69	1.22	0.76	0.89	1.17	
JCb-s1	A	1.00	0	23	2.00	1.00	0.24	0.10	0.07	0.78	0.76	0.97	0.99	0.97	0.98	
JCb-s2	A	1.00	0	23	2.00	1.00	0.24	0.10	0.15	0.69	0.80	1.17	0.90	1.02	1.14	
Karayannis et al. (1998)																
J2b	A	1.00	0	26	2.00	1.00	0.21	0.10	0.10	0.64	0.76	1.19	0.86	0.99	1.15	
J2(b)	A	1.00	0	22	2.00	1.00	0.17	0.10	0.12	0.56	0.67	1.18	0.76	0.87	1.14	
JO	A	1.00	0	21	2.00	1.00	0.18	0.10	0.00	0.65	0.46	0.71	0.85	0.65	0.77	

**Table 2** (continued)

Test ID	Type	$\alpha_{setup}$	CIR <sup>e</sup>	$f'_c$ (MPa)	$\frac{h_c}{b_c}$	$\alpha$	$r_B$	$r_N$	$\rho_{s,j}$	$P_{r,tot}^{exp}$	$P_{r,tot}$	$\frac{exp}{ana}$	$V_{jh}^{exp}$	$V_{jh}^{ana}$	$\frac{exp}{ana}$	
Del Vecchio et al. (2014)																
T_C1	A	1.00	0	13	1.67	1.67	0.25	0.20	0.00	0.39	0.36	0.92	0.66	0.62	0.95	
T_C1	A	1.00	0	13	1.67	1.67	0.15	0.20	0.00	0.30	0.32	1.08	0.54	0.57	1.05	
T_C2	A	1.00	0	16	1.67	1.67	0.19	0.20	0.00	0.44	0.35	0.81	0.74	0.64	0.87	
T_C2	A	1.00	0	16	1.67	1.67	0.12	0.20	0.00	0.31	0.31	0.99	0.60	0.59	1.00	
T_C3	A	1.00	0	16	1.67	1.67	0.19	0.20	0.00	0.46	0.35	0.77	0.76	0.64	0.84	
T_C3	A	1.00	0	16	1.67	1.67	0.12	0.20	0.00	0.35	0.31	0.89	0.64	0.59	0.92	
Di Ludovico et al. (2012)																
T-C2	A	1.00	0	19	1.67	1.67	0.16	0.20	0.00	0.35	0.35	1.00	0.65	0.65	1.00	
T-C2	A	1.00	0	19	1.67	1.67	0.10	0.20	0.00	0.28	0.31	1.10	0.57	0.61	1.06	
Kaya et al. (2008)																
3	A	1.18	0	14	2.00	2.00	0.13	0.40	0.00	0.11	0.23	2.15	0.37	0.62	1.66	
4	A	1.18	0	14	2.00	2.00	0.17	0.40	0.00	0.13	0.24	1.80	0.42	0.64	1.51	
Genesio and Sharma (2010)																
JT1-1	A	1.00	0	25	1.33	1.33	0.15	0.00	0.00	0.73	0.53	0.73	0.73	0.53	0.73	
JT5-1	A	1.00	0	28	1.33	1.33	0.07	0.00	0.00	0.46	0.42	0.92	0.46	0.42	0.92	
Genesio (2012)																
2D_bent_in	A	1.18	0	18	1.43	1.43	0.10	0.12	0.00	0.49	0.28	0.56	0.62	0.47	0.75	
2D_bent_125ar	A	1.18	0	18	1.25	1.25	0.16	0.12	0.00	0.53	0.31	0.58	0.65	0.50	0.77	
2D_bent_in_175ar	A	1.18	0	18	1.74	1.74	0.10	0.12	0.00	0.37	0.28	0.76	0.51	0.47	0.93	
2D_bent_in_2ar	A	1.18	0	18	2.00	2.00	0.10	0.12	0.00	0.32	0.29	0.90	0.46	0.48	1.04	
m7	A	1.00	0	29	1.33	1.33	0.08	0.00	0.00	0.50	0.44	0.88	0.50	0.44	0.88	
m8	A	1.00	0	29	1.33	1.33	0.09	0.00	0.00	0.52	0.45	0.86	0.52	0.45	0.86	
m18	A	1.00	0	60	1.33	1.33	0.04	0.00	0.00	0.43	0.42	0.96	0.43	0.42	0.96	
m19	A	1.00	0	60	1.33	1.33	0.05	0.00	0.00	0.48	0.44	0.91	0.48	0.44	0.91	

**Table 2** (continued)

Test ID	Type	$\alpha_{setup}$	CIR <sup>e</sup>	$f'_c$ (MPa)	$\frac{h_c}{b_c}$	$\alpha$	$r_B$	$r_N$	$\rho_{s,j}$	$P_{r,tot}^{exp}$	$P_{r,tot}$	$\frac{exp}{ana}$	$V_{jh}^{exp}$	$V_{jh}^{ana}$	$\frac{exp}{ana}$
m21	A	1.00	0	60	1.33	1.33	0.06	0.00	0.00	0.54	0.46	0.86	0.54	0.46	0.86
m22	A	1.00	0	60	1.33	1.33	0.06	0.00	0.00	0.55	0.47	0.86	0.55	0.47	0.86
m23	A	1.00	0	60	1.33	1.33	0.07	0.00	0.00	0.60	0.49	0.81	0.60	0.49	0.81
m25	A	1.00	0	29	1.33	1.33	0.05	0.00	0.00	0.42	0.39	0.94	0.42	0.39	0.94
m26	A	1.00	0	29	1.33	1.33	0.05	0.00	0.00	0.41	0.39	0.95	0.41	0.39	0.95
m27	A	1.00	0	29	1.33	1.33	0.05	0.00	0.00	0.41	0.39	0.95	0.41	0.39	0.95
m29	A	1.00	0	29	1.33	1.33	0.08	0.00	0.00	0.49	0.44	0.89	0.49	0.44	0.89
m30	A	1.00	0	29	1.33	1.33	0.08	0.00	0.00	0.51	0.44	0.86	0.51	0.44	0.86
m31	A	1.00	0	29	1.33	1.33	0.08	0.00	0.00	0.50	0.44	0.88	0.50	0.44	0.88
m32	A	1.00	0	29	1.33	1.33	0.08	0.00	0.00	0.51	0.44	0.86	0.51	0.44	0.86
m34	A	1.00	0	60	1.33	1.33	0.04	0.00	0.00	0.42	0.41	0.98	0.42	0.41	0.98
m35	A	1.00	0	60	1.33	1.33	0.04	0.00	0.00	0.41	0.41	1.00	0.41	0.41	1.00
m36	A	1.00	0	60	1.33	1.33	0.04	0.00	0.00	0.41	0.41	1.00	0.41	0.41	1.00
m38	A	1.00	0	29	1.33	1.33	0.12	0.00	0.00	0.77	0.50	0.64	0.77	0.50	0.64
m39	A	1.00	0	29	1.33	1.33	0.12	0.00	0.00	0.75	0.50	0.66	0.75	0.50	0.66
m40	A	1.00	0	60	1.33	1.33	0.06	0.00	0.00	0.53	0.46	0.87	0.53	0.46	0.87
m41	A	1.00	0	60	1.33	1.33	0.07	0.00	0.00	0.53	0.49	0.91	0.53	0.49	0.91
m47	A	1.00	0	29	1.33	1.33	0.06	0.00	0.00	0.45	0.41	0.90	0.45	0.41	0.90
m48	A	1.00	0	29	1.33	1.33	0.07	0.00	0.00	0.50	0.43	0.86	0.50	0.43	0.86
m49	A	1.00	0	29	1.33	1.33	0.10	0.00	0.00	0.59	0.47	0.80	0.59	0.47	0.80
JT4_roller_0N_neg	A	1.00	0	28	1.33	1.33	0.14	0.00	0.00	0.52	0.53	1.02	0.52	0.53	1.02
JT4_roller_150N_neg	A	1.00	0	28	1.33	1.33	0.14	0.05	0.00	0.47	0.43	0.92	0.60	0.56	0.94
JT4_roller_300N_neg	A	1.00	0	28	1.33	1.33	0.20	0.10	0.00	0.47	0.44	0.94	0.70	0.67	0.96
JT4_roller_450N_neg	A	1.00	0	28	1.33	1.33	0.20	0.15	0.00	0.39	0.41	1.04	0.70	0.72	1.03
JT4_roller_600N_neg	A	1.00	0	28	1.33	1.33	0.20	0.20	0.00	0.37	0.38	1.05	0.75	0.77	1.03

**Table 2** (continued)

Test ID	Type	$\alpha_{setup}$	CIR <sup>e</sup>	$f'_c$ (MPa)	$\frac{h_c}{b_c}$	$\alpha$	$r_B$	$r_N$	$\rho_{s,j}$	$P_{r,tot}^{exp}$	$P_{r,tot}$	$\frac{exp}{ana}$	$v_{jh}^{exp}$	$v_{jh}^{ana}$	$\frac{exp}{ana}$	
JT4_roller_900N_neg	A	1.00	0	28	1.33	1.33	0.20	0.30	0.00	0.34	0.34	0.99	0.84	0.84	1.00	
JT4_roller_1200N_neg	A	1.00	0	28	1.33	1.33	0.20	0.41	0.00	0.32	0.31	0.94	0.93	0.89	0.97	
JT4_20fc_neg	A	1.00	0	20	1.33	1.33	0.20	0.00	0.00	0.52	0.55	1.05	0.52	0.55	1.05	
JT4_40fc_neg	A	1.00	0	40	1.33	1.33	0.10	0.00	0.00	0.55	0.51	0.93	0.55	0.51	0.93	
JT4_50fc_neg	A	1.00	0	50	1.33	1.33	0.08	0.00	0.00	0.58	0.50	0.85	0.58	0.50	0.85	
JT16b_neg	A	1.00	0	28	1.33	1.33	0.10	0.00	0.00	0.51	0.47	0.93	0.51	0.47	0.93	
JT4_25b_neg	A	1.00	0	28	1.33	1.33	0.25	0.00	0.00	0.57	0.66	1.15	0.57	0.66	1.15	
JT4_25_4b_neg	A	1.00	0	28	1.33	1.33	0.33	0.00	0.00	0.63	0.75	1.19	0.63	0.75	1.19	
JT4_12c_neg	A	1.00	0	28	1.33	1.33	0.14	0.00	0.00	0.55	0.53	0.97	0.55	0.53	0.97	
JT4_16c_neg	A	1.00	0	28	1.33	1.33	0.14	0.00	0.00	0.53	0.53	1.00	0.53	0.53	1.00	
JT4_25c_neg	A	1.00	0	28	1.33	1.33	0.14	0.00	0.00	0.51	0.53	1.04	0.51	0.53	1.04	
JT+B198: B2424_25_4c_neg	A	1.00	0	28	1.33	1.33	0.14	0.00	0.00	0.52	0.53	1.03	0.52	0.53	1.03	
Helal (2012)																
JA-1	A	1.00	1	23	1.54	1.54	0.20	0.10	0.00	0.35	0.50	1.42	0.53	0.69	1.29	
JA-2	A	1.00	1	31	1.54	1.54	0.15	0.12	0.00	0.32	0.47	1.46	0.56	0.73	1.30	
JA-3	A	1.00	1	29	1.54	1.54	0.16	0.08	0.00	0.37	0.50	1.38	0.53	0.68	1.27	
JA-4	A	1.00	1	29	1.54	1.54	0.16	0.08	0.00	0.35	0.50	1.42	0.52	0.68	1.30	
Liu (2006)																
RC-1	A	1.18	0	19	1.65	1.43	0.12	0.07	0.00	0.54	0.33	0.61	0.60	0.46	0.77	
Kim et al. (2016)																
ER1	A	1.18	0	20	1.37	1.37	0.34	0.00	0.06	0.95	0.86	0.90	0.81	0.86	1.06	
ER2	A	1.18	0	20	1.37	1.37	0.17	0.00	0.06	0.52	0.63	1.23	0.44	0.63	1.45	
EU1	A	1.18	0	20	1.37	1.37	0.34	0.00	0.06	0.96	0.86	0.89	0.82	0.86	1.05	
EU1	A	1.18	0	20	1.37	1.37	0.17	0.00	0.06	0.68	0.63	0.94	0.57	0.63	1.10	
ER2	A	1.18	0	31	1.37	1.37	0.22	0.00	0.08	1.24	0.82	0.66	1.05	0.82	0.78	

**Table 2** (continued)

Test ID	Type	$\alpha_{setup}$	CIR <sup>e</sup>	$f'_c$ (MPa)	$\frac{h_c}{b_c}$	$\alpha$	$r_B$	$r_N$	$\rho_{s,j}$	$P_{r,tot}^{exp}$	$P_{r,tot}^{ana}$	$\frac{exp}{ana}$	$v_{jh}^{exp}$	$v_{jh}^{ana}$	$\frac{exp}{ana}$	
ER2	A	1.18	0	31	1.37	1.37	0.13	0.00	0.08	1.02	0.65	0.63	0.87	0.65	0.75	
EU2	A	1.18	0	31	1.37	1.37	0.22	0.00	0.08	1.26	0.82	0.65	1.07	0.82	0.77	
EU2	A	1.18	0	31	1.37	1.37	0.13	0.00	0.08	1.05	0.65	0.62	0.89	0.65	0.73	
EU2C	A	1.18	0	31	1.37	1.07	0.22	0.00	0.07	1.37	0.86	0.63	1.16	0.86	0.74	
EU2C	A	1.18	0	31	1.37	1.07	0.13	0.00	0.07	0.87	0.67	0.77	0.74	0.67	0.91	
EN	A	1.18	0	20	1.37	1.37	0.34	0.00	0.00	0.64	0.58	0.91	0.54	0.58	1.07	
EN	A	1.18	0	20	1.37	1.37	0.17	0.00	0.00	0.47	0.45	0.95	0.40	0.45	1.12	
Pantelides et al. (2002)																
1	B <sup>b</sup>	1.00	0	33	1.00	1.00	0.22	0.10	0.00	0.25	0.14	0.55	0.45	0.31	0.69	
2	B	1.00	0	30	1.00	1.00	0.24	0.27	0.00	0.24	0.12	0.48	0.65	0.43	0.67	
Dhake et al. (2015)																
J1	B	1.00	0	30	1.20	0.90	0.15	0.11	0.00	0.17	0.26	1.56	0.36	0.48	1.32	
Sasmal (2009)																
SP-1	B	1.00	0	30	1.33	1.33	0.08	0.11	0.02	0.18	0.24	1.29	0.38	0.45	1.17	
Murty et al. (2003)																
S1	B	1.00	1	28	2.00	1.60	0.12	0.00	0.00	0.45	0.41	0.92	0.45	0.41	0.92	
S2	B	1.00	1	27	2.00	1.60	0.12	0.00	0.03	0.81	0.59	0.73	0.81	0.59	0.73	
S3	B	1.00	1	30	2.00	1.60	0.11	0.00	0.02	0.62	0.58	0.93	0.62	0.58	0.93	
El-Amoury (2003)																
T-B10	B	1.00	1	34	1.60	1.00	0.08	0.18	0.08	0.14	0.22	1.53	0.41	0.52	1.27	
T-SB3	B	1.00	1	31	1.60	1.00	0.19	0.20	0.00	0.19	0.15	0.77	0.50	0.43	0.86	
Shafaei et al. (2014)																
J3	B	1.00	1	25	1.14	1.00	0.16	0.14	0.00	0.17	0.13	0.74	0.40	0.33	0.84	
Parvin et al. (2010)																
U.S.2	B	1.18	0	25	1.67	1.67	0.07	0.31	0.00	0.06	0.10	1.59	0.30	0.41	1.39	



**Table 2** (continued)

Test ID	Type	$\alpha_{setup}$	CIR <sup>e</sup>	$f'_c$ (MPa)	$\frac{h_c}{b_c}$	$\alpha$	$r_B$	$r_N$	$\rho_{s,j}$	$P_{r,tot}^{exp}$	$P_{r,tot}$	$\frac{exp}{ana}$	$v_{jh}^{exp}$	$v_{jh}^{ana}$	$\frac{exp}{ana}$	
U.S.3	B	1.18	0	25	1.67	1.67	0.07	0.31	0.00	0.07	0.10	1.45	0.31	0.41	1.32	
U.S.4	B	1.18	0	25	1.67	1.67	0.07	0.16	0.00	0.09	0.11	1.17	0.26	0.31	1.20	
Biddah (1997)																
J4	B	1.18	1	24	1.00	1.20	0.07	0.07	0.02	0.20	0.17	0.89	0.29	0.30	1.04	
Genesis and Sharma (2010)																
JT3-1	B	1.00	0	28	1.33	1.33	0.14	0.00	0.00	0.35	0.26	0.73	0.35	0.26	0.73	
Gergely et al. (2000)																
1	C <sup>c</sup>	1.00	0	20	1.14	1.00	0.28	0.00	0.00	0.28	0.38	1.37	0.28	0.38	1.37	
2	C	1.00	0	20	1.14	1.00	0.28	0.00	0.00	0.31	0.38	1.24	0.31	0.38	1.24	
10	C	1.00	0	34	1.14	1.00	0.16	0.00	0.00	0.21	0.36	1.71	0.21	0.36	1.71	
11	C	1.00	0	34	1.14	1.00	0.16	0.00	0.00	0.25	0.36	1.46	0.25	0.36	1.46	
Hakuto et al. (2000)																
O7	C	1.18	0	31	1.67	1.09	0.09	0.00	0.00	0.32	0.34	1.05	0.27	0.34	1.24	
O7	C	1.18	0	31	1.67	1.09	0.06	0.00	0.00	0.27	0.30	1.08	0.23	0.30	1.28	
Genesis and Sharma (2010)																
JT4-1	C	1.00	0	28	1.33	1.33	0.14	0.00	0.00	0.37	0.32	0.87	0.37	0.32	0.87	
Genesis (2012)																
JT4_20fc	C	1.00	0	20	1.33	1.33	0.19	0.00	0.00	0.35	0.33	0.95	0.35	0.33	0.95	
JT4_40fc	C	1.00	0	40	1.33	1.33	0.10	0.00	0.00	0.34	0.31	0.90	0.34	0.31	0.90	
JT4_50fc	C	1.00	0	50	1.33	1.33	0.08	0.00	0.00	0.39	0.30	0.77	0.39	0.30	0.77	
JT4_16b	C	1.00	0	28	1.33	1.33	0.10	0.00	0.00	0.35	0.29	0.82	0.35	0.29	0.82	
JT4_25b	C	1.00	0	28	1.33	1.33	0.24	0.00	0.00	0.38	0.40	1.06	0.38	0.40	1.06	
JT4_25_4b	C	1.00	0	28	1.33	1.33	0.32	0.00	0.00	0.40	0.45	1.12	0.40	0.45	1.12	
JT4_16c	C	1.00	0	28	1.33	1.33	0.14	0.00	0.00	0.35	0.32	0.90	0.35	0.32	0.90	
JT4_16c	C	1.00	0	28	1.33	1.33	0.14	0.00	0.00	0.34	0.32	0.93	0.34	0.32	0.93	

**Table 2** (continued)

Test ID	Type	$\alpha_{setup}$	CIR <sup>e</sup>	$f'_c$ (MPa)	$\frac{h_c}{b_c}$	$\alpha$	$r_B$	$r_N$	$\rho_{s,j}$	$P_{r,tot}^{exp}$	$P_{r,tot}$	$\frac{exp}{ana}$	$v_{jh}^{exp}$	$v_{jh}^{ana}$	$\frac{exp}{ana}$
JT4_25c	C	1.00	0	28	1.33	1.33	0.14	0.00	0.00	0.37	0.32	0.86	0.37	0.32	0.86
JT4_25_4c	C	1.00	0	28	1.33	1.33	0.14	0.00	0.00	0.37	0.32	0.88	0.37	0.32	0.88
JT2_rol1_150N	C	1.00	0	28	1.33	1.33	0.14	0.05	0.00	0.27	0.26	0.98	0.38	0.38	0.99
JT2_rol1_300N	C	1.00	0	28	1.33	1.33	0.14	0.10	0.00	0.25	0.24	0.97	0.45	0.44	0.98
JT2_rol1_450N	C	1.00	0	28	1.33	1.33	0.14	0.15	0.00	0.28	0.22	0.80	0.56	0.49	0.87
JT2_rol1_600N	C	1.00	0	28	1.33	1.33	0.14	0.20	0.00	0.27	0.21	0.77	0.62	0.54	0.86
JT2_rol1_900N	C	1.00	0	28	1.33	1.33	0.14	0.30	0.00	0.28	0.19	0.69	0.74	0.60	0.81
JT2_rol1_1200N	C	1.00	0	28	1.33	1.33	0.14	0.41	0.00	0.28	0.17	0.61	0.86	0.66	0.77
JT4_350ar	C	1.00	0	28	1.17	1.17	0.14	0.00	0.00	0.37	0.31	0.85	0.37	0.31	0.85
JT4_500ar	C	1.00	0	28	1.67	1.67	0.14	0.00	0.00	0.37	0.33	0.91	0.37	0.33	0.91
JT4_600ar	C	1.00	0	28	2.00	2.00	0.14	0.00	0.00	0.35	0.34	0.97	0.35	0.34	0.97
JT4_10BJ	C	1.00	0	50	1.33	1.33	0.06	0.00	0.00	0.32	0.27	0.85	0.32	0.27	0.85
JT4_20BJ	C	1.00	0	28	1.33	1.33	0.07	0.00	0.00	0.30	0.25	0.85	0.30	0.25	0.85
JT4_30BJ	C	1.00	0	28	1.33	1.33	0.07	0.00	0.00	0.29	0.25	0.88	0.29	0.25	0.88
JT4_40BJ	C	1.00	0	28	1.33	1.33	0.06	0.00	0.00	0.28	0.24	0.87	0.28	0.24	0.87
2D_bent_out	C	1.18	0	18	1.43	1.43	0.10	0.12	0.00	0.28	0.17	0.62	0.42	0.34	0.82
2D_bent_out_1ar	C	1.18	0	18	1.00	1.00	0.16	0.12	0.00	0.42	0.18	0.44	0.55	0.35	0.65
2D_bent_out_125ar	C	1.18	0	18	1.25	1.25	0.16	0.12	0.00	0.33	0.19	0.57	0.47	0.36	0.77
2D_bent_out_175ar	C	1.18	0	18	1.74	1.74	0.10	0.12	0.00	0.36	0.17	0.49	0.49	0.34	0.70
2D+B282:B309_bent_out_2ar	C	1.18	0	18	2.00	2.00	0.10	0.12	0.00	0.35	0.18	0.51	0.49	0.35	0.71
Chun et al. (2007)															
JC-2	C	1.00	1	60	1.43	1.00	0.09	0.03	0.01	0.33	0.46	1.39	0.46	0.59	1.30
JC-No. 11-1	C	1.00	1	33	1.12	0.97	0.19	0.00	0.03	0.65	0.65	1.00	0.65	0.65	1.00

**Table 2** (continued)

Test ID	Type	$\alpha_{setup}$	CIR <sup>e</sup>	$f'_c$ (MPa)	$\frac{h_c}{b_c}$	$\alpha$	$r_B$	$r_N$	$\rho_{s,j}$	$P_{t,tot}^{exp}$	$P_{t,tot}^{ana}$	$\frac{exp}{ana}$	$V_{jt}^{exp}$	$V_{jt}^{ana}$	$\frac{exp}{ana}$
Chun and Kim (2004)															
JC-2	C	1.00	0	60	1.43	1.00	0.09	0.03	0.01	0.39	0.39	1.00	0.52	0.52	1.00
Wong (2005)															
BS-LL	C	1.00	0	42	1.73	1.50	0.10	0.15	0.00	0.18	0.23	1.26	0.47	0.54	1.15
BS-OL	C	1.00	0	31	1.73	1.50	0.14	0.15	0.00	0.20	0.24	1.20	0.47	0.52	1.11
De Risi et al. (2016a, b)															
1	D <sup>d</sup>	1.00	0	29	1.67	1.67	0.10	0.10	0.00	0.35	0.31	0.86	0.56	0.51	0.90
2	D	1.00	0	29	1.67	1.67	0.05	0.10	0.00	0.19	0.25	1.31	0.37	0.45	1.19
De Risi and Verderame (2017)															
#1bP	D	1.00	0	18	1.33	1.33	0.22	0.10	0.00	0.44	0.34	0.76	0.62	0.51	0.82
#2bP	D	1.00	0	18	1.33	1.33	0.12	0.10	0.00	0.43	0.29	0.68	0.60	0.45	0.75
#1cP	D	1.00	0	18	2.00	2.00	0.15	0.10	0.00	0.32	0.32	0.98	0.49	0.48	0.98
#2cP	D	1.00	0	18	2.00	2.00	0.08	0.10	0.00	0.19	0.27	1.46	0.34	0.44	1.29
Melo et al. (2012)															
TPC	D	1.18	0	24	1.60	1.60	0.06	0.13	0.00	0.28	0.21	0.76	0.46	0.43	0.93
Genesio and Sharma (2010)															
JT2-1	D	1.00	0	24	1.33	1.33	0.09	0.00	0.00	0.40	0.36	0.89	0.40	0.36	0.89
Genesio (2012)															
JT2_test_20fc	D	1.00	0	20	1.33	1.33	0.11	0.00	0.00	0.43	0.37	0.84	0.43	0.37	0.84
JT2_test_30fc	D	1.00	0	30	1.33	1.33	0.07	0.00	0.00	0.43	0.35	0.82	0.43	0.35	0.82
JT2_test_40fc	D	1.00	0	40	1.33	1.33	0.05	0.00	0.00	0.13	0.34	2.68	0.43	0.34	0.79
JT2_test_50fc	D	1.00	0	50	1.33	1.33	0.04	0.00	0.00	0.40	0.33	0.83	0.40	0.33	0.83
JT2_16b	D	1.00	0	24	1.33	1.33	0.06	0.00	0.00	0.40	0.32	0.81	0.40	0.32	0.81
JT2_25b	D	1.00	0	24	1.33	1.33	0.16	0.00	0.00	0.46	0.44	0.95	0.46	0.44	0.95
JT2_25_4b	D	1.00	0	24	1.33	1.33	0.21	0.00	0.00	0.49	0.49	0.98	0.49	0.49	0.98

**Table 2** (continued)

Test ID	Type	$\alpha_{setup}$	CIR <sup>e</sup>	$f'_c$ (MPa)	$\frac{h_c}{b_c}$	$\alpha$	$r_B$	$r_N$	$\rho_{s,j}$	$P_{r,rot}^{exp}$	$P_{r,rot}^{ana}$	$\frac{exp}{ana}$	$v_{jh}^{exp}$	$v_{jh}^{ana}$	$\frac{exp}{ana}$
JT2_12c	D	1.00	0	24	1.33	1.33	0.09	0.00	0.00	0.42	0.36	0.85	0.42	0.36	0.85
JT2_16c	D	1.00	0	24	1.33	1.33	0.09	0.00	0.00	0.41	0.36	0.86	0.41	0.36	0.86
JT2_25c	D	1.00	0	24	1.33	1.33	0.09	0.00	0.00	0.41	0.36	0.86	0.41	0.36	0.86
JT2_25_4c	D	1.00	0	24	1.33	1.33	0.09	0.00	0.00	0.42	0.36	0.86	0.42	0.36	0.86
JT2_rol1_150N	D	1.00	0	24	1.33	1.33	0.09	0.06	0.00	0.34	0.30	0.87	0.47	0.42	0.90
JT2_rol1_300N	D	1.00	0	24	1.33	1.33	0.09	0.12	0.00	0.30	0.27	0.90	0.53	0.49	0.93
JT2_rol1_450N	D	1.00	0	24	1.33	1.33	0.09	0.18	0.00	0.31	0.26	0.84	0.62	0.55	0.90
JT2_rol1_600N	D	1.00	0	24	1.33	1.33	0.09	0.23	0.00	0.31	0.24	0.79	0.69	0.60	0.87
JT2_rol1_900N	D	1.00	0	24	1.33	1.33	0.09	0.35	0.00	0.30	0.22	0.74	0.81	0.68	0.84
JT2_rol1_1200N	D	1.00	0	24	1.33	1.33	0.09	0.47	0.00	0.28	0.21	0.73	0.88	0.74	0.84
JT2_rol1_300N	D	1.00	0	24	1.33	1.33	0.21	0.06	0.00	0.39	0.38	0.98	0.52	0.52	0.98
JT2_rol1_450N	D	1.00	0	24	1.33	1.33	0.21	0.12	0.00	0.33	0.34	1.05	0.56	0.58	1.03
JT2_rol1_600N	D	1.00	0	24	1.33	1.33	0.21	0.18	0.00	0.32	0.32	1.00	0.63	0.63	1.00
JT2_rol1_900N	D	1.00	0	24	1.33	1.33	0.21	0.23	0.00	0.31	0.30	0.95	0.70	0.67	0.97
JT2_350ar	D	1.00	0	24	1.17	1.17	0.09	0.00	0.00	0.43	0.35	0.81	0.43	0.35	0.81
JT2_500ar	D	1.00	0	24	1.67	1.67	0.09	0.00	0.00	0.29	0.37	1.29	0.29	0.37	1.29
JT2_600ar	D	1.00	0	24	2.00	2.00	0.09	0.00	0.00	0.25	0.38	1.51	0.25	0.38	1.51
JT2_10BJ	D	1.00	0	30	1.33	1.33	0.07	0.00	0.00	0.40	0.35	0.87	0.40	0.35	0.87
JT2_11BJ	D	1.00	0	30	1.33	1.33	0.06	0.00	0.00	0.38	0.34	0.89	0.38	0.34	0.89
JT2_20BJ	D	1.00	0	24	1.33	1.33	0.08	0.00	0.00	0.39	0.34	0.88	0.39	0.34	0.88
JT2_30BJ	D	1.00	0	24	1.33	1.33	0.07	0.00	0.00	0.38	0.34	0.89	0.38	0.34	0.89
Akgezul and Pampanin (2010)															
2DB1	D	1.18	0	25	1.43	1.43	0.06	0.04	0.01	0.28	0.28	1.03	0.31	0.37	1.17
2DB1	D	1.18	0	25	1.43	1.43	0.06	0.08	0.01	0.24	0.26	1.12	0.35	0.42	1.21
2DB2	D	1.18	0	18	1.43	1.43	0.10	0.21	0.00	0.22	0.21	0.96	0.45	0.48	1.08
2DB2	D	1.18	0	18	1.43	1.43	0.10	0.05	0.00	0.31	0.25	0.81	0.35	0.34	0.97

**Table 2** (continued)

Test ID	Type	$\alpha_{setup}$	CIR <sup>e</sup>	$f'_c$ (MPa)	$\frac{h_c}{b_b}$	$\alpha$	$r_B$	$r_N$	$\rho_{s,j}$	$P_{t,lot}^{exp}$	$P_{t,lot}$	$\frac{exp}{ana}$	$v_{j,h}^{exp}$	$v_{j,h}^{ana}$	$\frac{exp}{ana}$	
Genesio (2012)																
3_2D	D	1.18	0	18	1.43	1.43	0.10	0.12	0.00	0.29	0.23	0.78	0.43	0.41	0.95	
4_2D	D	1.18	0	18	1.43	1.43	0.10	0.24	0.00	0.27	0.20	0.75	0.53	0.50	0.93	
13_2D	D	1.18	0	18	1.43	1.43	0.14	0.12	0.00	0.29	0.25	0.85	0.43	0.43	1.00	
14_2D	D	1.18	0	18	1.43	1.43	0.20	0.12	0.00	0.33	0.27	0.83	0.47	0.46	0.99	
15_2D	D	1.18	0	18	1.43	1.43	0.26	0.12	0.00	0.32	0.29	0.91	0.46	0.48	1.05	
16_2D	D	1.18	0	18	1.43	1.43	0.40	0.12	0.00	0.32	0.34	1.07	0.46	0.54	1.18	
17_2D	D	1.18	0	18	1.43	1.43	0.06	0.12	0.00	0.27	0.21	0.78	0.41	0.38	0.95	
18_2D	D	1.18	0	18	1.43	1.43	0.10	0.12	0.00	0.34	0.23	0.68	0.47	0.41	0.86	
19_2D	D	1.18	0	18	1.43	1.43	0.10	0.12	0.00	0.34	0.23	0.66	0.48	0.41	0.85	
20_2D	D	1.18	0	18	1.43	1.43	0.10	0.12	0.00	0.34	0.23	0.68	0.47	0.41	0.86	
21_2D	D	1.18	0	18	1.43	1.43	0.10	0.12	0.00	0.33	0.23	0.69	0.47	0.41	0.87	
22_2D	D	1.18	0	18	1.43	1.43	0.10	0.12	0.00	0.25	0.23	0.92	0.39	0.41	1.06	
24_2D	D	1.18	0	18	1.43	1.43	0.23	0.18	0.00	0.30	0.26	0.87	0.51	0.52	1.02	
25_2D	D	1.18	0	18	1.43	1.43	0.23	0.36	0.00	0.23	0.22	0.93	0.58	0.61	1.05	
30_2D	D	1.18	0	12	1.43	1.43	0.15	0.08	0.00	0.32	0.25	0.77	0.39	0.36	0.94	
31_2D	D	1.18	0	28	1.43	1.43	0.06	0.03	0.00	0.31	0.25	0.81	0.33	0.32	0.96	
32_2D	D	1.18	0	33	1.43	1.43	0.05	0.04	0.00	0.28	0.24	0.89	0.33	0.34	1.03	
33_2D	D	1.18	0	38	1.43	1.43	0.05	0.05	0.00	0.24	0.24	0.99	0.32	0.36	1.11	
34_2D	D	1.18	0	43	1.43	1.43	0.04	0.05	0.00	0.22	0.23	1.06	0.31	0.36	1.17	
35_2D	D	1.18	0	24	1.43	1.43	0.07	0.03	0.00	0.34	0.25	0.75	0.35	0.32	0.91	
39_2D	D	1.18	0	18	1.43	1.43	0.10	0.02	0.00	0.37	0.27	0.73	0.35	0.31	0.88	
I_2D_1ar	D	1.18	0	18	1.00	1.00	0.10	0.11	0.00	0.30	0.22	0.75	0.42	0.39	0.92	
I_2D_125ar	D	1.18	0	18	1.25	1.25	0.10	0.11	0.00	0.38	0.23	0.60	0.50	0.40	0.79	

**Table 2** (continued)

Test ID	Type	$\alpha_{setup}$	CIR <sup>e</sup>	$f'_c$ (MPa)	$\frac{h_c}{b_c}$	$\alpha$	$r_B$	$r_N$	$\rho_{sj}$	$P_{r,tot}^{exp}$	$P_{r,tot}$	$\frac{exp}{ana}$	$v_{jh}^{exp}$	$v_{jh}^{ana}$	$\frac{exp}{ana}$	
L_2D_175ar	D	1.18	0	18	1.74	1.74	0.10	0.11	0.00	0.25	0.24	0.96	0.37	0.41	1.09	
L_2D_2ar	D	1.18	0	18	2.00	2.00	0.10	0.11	0.00	0.21	0.24	1.14	0.34	0.41	1.21	
Pampanin et al. (2007)																
T1	D	1.18	0	24	1.65	1.65	0.07	0.13	0.00	0.21	0.22	1.07	0.38	0.44	1.16	
T1	D	1.18	0	24	1.65	1.65	0.07	0.08	0.00	0.22	0.24	1.09	0.33	0.39	1.19	
T2	D	1.18	0	24	1.65	1.65	0.07	0.13	0.00	0.21	0.22	1.06	0.38	0.44	1.15	
T2	D	1.18	0	24	1.65	1.65	0.07	0.08	0.00	0.22	0.24	1.07	0.33	0.39	1.17	
Kam (2010)																
NS-OI	D	1.18	0	17	1.43	1.43	0.09	0.22	0.00	0.24	0.20	0.83	0.48	0.47	0.99	
NS-OI	D	1.18	0	17	1.43	1.43	0.09	0.05	0.00	0.34	0.24	0.72	0.38	0.33	0.88	
S-OI	D	1.18	0	15	1.43	1.43	0.09	0.24	0.00	0.22	0.20	0.89	0.46	0.47	1.03	
S-OI	D	1.18	0	15	1.43	1.43	0.09	0.06	0.00	0.33	0.23	0.70	0.39	0.33	0.87	
Hertanto (2005)																
TDP-1	D	1.18	0	23	1.50	1.30	0.08	0.09	0.01	0.33	0.29	0.89	0.45	0.46	1.03	
TDP-2	D	1.18	0	25	1.50	1.30	0.07	0.08	0.01	0.31	0.29	0.93	0.42	0.45	1.07	
TDP-2	D	1.18	0	25	1.50	1.30	0.03	0.04	0.01	0.35	0.26	0.73	0.38	0.34	0.89	
Laterza et al. (2017)																
T23	D	1	0	14	1.65	1.65	0.15	0.15	0.00	0.32	0.24	0.76	0.48	0.44	0.93	
											Mean	0.988				
											SD	0.27				
											MAPE	19.4%				

<sup>a</sup>Joints with 90°-hook bent into the core

<sup>b</sup>Joints with straight anchorage into the joint core

<sup>c</sup>Joints with 90°-hook bent out the core

<sup>d</sup>Joints with 180°-hook; CIR denotes the column intermediate reinforcement

<sup>e</sup>denotes CIR = 1 and 0 for RC joints with and without column intermediate reinforcement, respectively

## References

- ACI 352R-02 (2002) Recommendations for design of beam–column-joints in monolithic reinforced concrete structures. American Concrete Institute, ACI ASCE, Committee 352, Detroit
- Akguzel U, Pampanin S (2010) Effects of variation of axial load and bi-directional loading on seismic performance of GFRP retrofitted reinforced concrete exterior beam–column joints. *J Compos Constr* 14(1):94–104
- Akguzel U, Pampanin S (2012) Assessment and design procedure for the seismic retrofit of reinforced concrete beam–column joints using FRP composite materials. *J Compos Constr* 16:21–34
- Alva GMS, De Cresce El Debs ALH, El Debs MK (2007) An experimental study on cyclic behaviour of reinforced concrete connections. *Can J Civ Eng* 34(4):565–575
- Antonopoulos CP, Triantafyllou TC (2003) Experimental investigation of FRP strengthened RC beam column joints. *J Compos Constr* 7:39–49
- Biddah MSA (1997) Seismic behaviour of existing and rehabilitated reinforced concrete frame connections. Ph.D. dissertation, McMaster University, Ontario
- Campione G, Cavaleri L, Failla A (2016) Flexural behavior of external beam–column reinforced concrete assemblages externally strengthened with steel cages. *ACI Struct J* 113(5):883
- Chalioris CE, Favvata M, Karayannis CG (2008) Reinforced concrete beam–column joints with crossed inclined bars under cyclic deformations. *J Earthq Eng Struct Dyn* 37:881–897
- Chun SC, Lee SH, Kang TH, Oh B, Wallace JW (2007) Mechanical anchorage in exterior beam–column joints subjected to cyclic loading. *ACI Struct J* 104(1):102
- Chun SC, Kim, DY (2004) Evaluation of mechanical anchorage of reinforcement by exterior beam–column joint experiments. In: Proceedings of 13th world conference on earthquake engineering (No. 0326)
- Clyde C, Pantelides CP, Reaveley LD (2000) Performance-based evaluation of exterior reinforced concrete building joints for seismic excitation. Report PEER 2000/05. Pacific Earthquake Engineering Research Center
- Computer and Structures Inc (2008) SAP2000 analysis references. Computer and Structures Inc, Berkeley
- De Risi MT, Verderame GM (2017) Experimental assessment and numerical modelling of exterior non-conforming beam–column joints with plain bars. *Eng Struct* 150:115–134
- De Risi MT, Ricci P, Verderame GM, Manfredi G (2016a) Experimental assessment of unreinforced exterior beam–column joints with deformed bars. *Eng Struct* 112:215–232
- De Risi MT, Ricci P, Verderame GM (2016b) Modelling exterior unreinforced beam–column joints in seismic analysis of non-ductile RC frames. *J Earthq Eng Struct Dyn* 46(6):899–923
- Del Vecchio C, Di Ludovico M, Balsamo A, Protà A, Manfredi G, Dolce M (2014) Experimental investigation of exterior RC beam–column joints retrofitted with FRP systems. *J Compos Constr* 18:1–13
- Del Vecchio C, Di Ludovico M, Protà A, Manfredi G (2016) Modelling beam–column joints and FRP strengthening in the seismic performance assessment of RC existing frames. *Compos Struct* 142:107–116
- Del Vecchio C, Gentile ER, Pampanin S (2017) The simplified lateral mechanism analysis (SLaMa) for the seismic performance assessment of a case study building damaged in the 2011 Christchurch earthquake. Research Report 2016-02 Civil and Natural Resources Engineering
- Dhake PD, Patil HS, Patil YD (2015) Anchorage behaviour and development length of headed bars in exterior beam–column joints. *Mag Concr Res* 67(2):53–62
- Di Ludovico M, Balsamo A, Protà A, Verderame GM, Dolce M, Manfredi G (2012) Preliminary results of an experimental investigation on RC beam–column joints. International Institute for FRP in Construction, Rome, pp 1–9
- Ehsani MR, Moussa AE, Valenilla CR (1987) Comparison of inelastic behavior of reinforced ordinary- and high-strength concrete frames. *ACI Struct J* 84(2):161–169
- El-Amoury T (2003) Seismic rehabilitation of concrete frame beam–column joints. Ph.D. dissertation, McMaster University, Ontario
- Elwood K (2002) Shake table tests and analytical studies on the gravity load collapse of reinforced concrete frames. Ph.D. Dissertation. University of California, Berkeley, California
- Favvata MJ, Izzuddin BA, Karayannis CG (2008) Modelling exterior beam–column joints for seismic analysis of RC frame structures. *J Earthq Eng Struct Dyn* 37(13):1527–1548
- García R, Jemaa Y, Helal Y, Maurizio G, Pilakoutas K (2013) Seismic strengthening of severely damaged beam–column RC joints using CFRP. *J Comps Constr* 18(2):04013048
- Genesio G (2012) Seismic assessment of RC exterior beam–column joints and retrofit with haunches using post-installed anchors. Ph.D. Dissertation. University of Stuttgart, Stuttgart

- Genesio G, Sharma A (2010) Seismic retrofit solution for reinforced concrete exterior beam–column joints using a fully fastened haunch: Part 2-1—as-built joints. IWB, University of Stuttgart, Stuttgart, Test Report No. WS 221/07-10/01
- Gergely BJ, Pantelides CP, Reveley LD (2000) Shear strengthening RCT-joints using CFRP composites. *J Compos Constr* 4:56–64
- Ghobarah A, Said A (2001) Seismic rehabilitation of beam–column joints using FRP laminates. *J Earthq Eng* 5(1):113–129
- Ha GJ, Cho CG, Kang HW, Feo L (2013) Seismic improvement of RC beam–column joints using hexagonal CFRP bars combined with CFRP sheets. *Compos Struct* 95:464–470
- Hadi MN, Tran TM (2016) Seismic rehabilitation of reinforced concrete beam–column joints by bonding with concrete covers and wrapping with FRP composites. *Mater Struct* 49(1–2):467–485
- Hakuto S, Park R, Tanaka H (2000) Seismic load tests on interior and exterior beam–column joints with substandard reinforcing details. *ACI Struct J* 97(1):11–25
- Hamil SJ (2000) Reinforced Concrete Beam–column Connection Behaviour. Ph.D. dissertation, Durham University, Durham
- Hassan WM (2011) Analytical and experimental assessment of seismic vulnerability of beam–column joints without transverse reinforcement in concrete buildings. Ph.D. Dissertation. University of California, Berkeley, California
- Helal Y (2012) Seismic strengthening of deficient exterior RC beam–column sub-assemblages using posttensioned metal strips. Ph.D. dissertation, University of Sheffield, Sheffield
- Hertanto E (2005) Seismic assessment of pre-1970s reinforced concrete structures. Master Thesis. University of Canterbury, Christchurch
- Hwang SJ, Lee HJ, Liao TF, Wang KC, Tsai HH (2005) Role of hoops on shear strength of reinforced concrete beam–column joints. *ACI Struct J* 102(3):445–453
- Jeon JS, Lowes LN, DesRoches R, Brilakis I (2015) Fragility curves for non-ductile reinforced concrete frames that exhibit different component response mechanisms. *Eng Struct* 85:127–143
- Kaku T, Asakusa H (1991) Ductility estimation of exterior beam–column subassemblages in reinforced concrete frames. ACI Special Publication, Design of Beam–column Joints for Seismic Resistance, ACI, Farmington Hills, pp 167–186
- Kam WY (2010) Selective Weakening and Post-tensioning for the Seismic Retrofit of Non-Ductile RC Frames. Ph.D. Dissertation. University of Canterbury, Christchurch
- Kang TH, Ha SS, Choi DU (2010) Bar pullout tests and seismic tests of small-headed bars in beam–column joints. *ACI Struct J* 107(1):32
- Karayannis CG, Sirkelis G (2008) Strengthening and rehabilitation of RC beam–column joints using carbon-FRP jacketing and epoxy resin injection. *J Earthq Eng Struct Dyn* 37(5):769–790
- Karayannis CG, Chalioris CE, Sideris KK (1998) Effectiveness of RC beam–column connection repair using epoxy resin injections. *J Earthq Eng* 2(2):217–240
- Karayannis CG, Chalioris CE, Sirkelis GM (2008) Local retrofit of external RC beam column joints using thin RC jackets: an experimental study. *J Earthq Eng Struct Dyn* 37(5):727–746
- Kaya O, Yalcin C, Parvin A, Altay S (2008) Repairing of shear-damaged RC joint panel zone using chemical epoxy injection methodology. In: Proceedings of 14th world conference on earthquake engineering, Beijing
- Kim CG, Eom TS, Park HG, Kim TW (2016) Seismic performance of lightly reinforced concrete beam–column connections for low-rise buildings. *J Arch Inst Korea Struct Constr* 32(3):19–30
- Kuang JS, Wong HF (2013) Horizontal hoops in non-seismically designed beam–column joints. *HKIE Trans* 20(3):164–171
- Laterza M, D'Amato M, Gigliotti R (2017) Modelling of gravity-designed RC sub-assemblages subjected to lateral loads. *Eng Struct* 130:242–260
- Le-Trung K, Lee K, Lee J, Lee DH, Woo S (2010) Experimental study of RC beam–column joints strengthened using CFRP composites. *Compos Part B Eng* 41(1):76–85
- Liu C (2006) Seismic behaviour of beam–column joint subassemblies reinforced with steel fibers. Master Thesis. University of Canterbury, Christchurch
- Lowes LN, Altoontash A (2003) Modelling reinforced-concrete beam–column joints subjected to cyclic loading. *J Struct Eng* 129:1686–1697
- Lynn AC (2001) Seismic evaluation of existing reinforced concrete building columns. Ph.D. Dissertation. University of California, Berkeley, California
- Melo J, Varum H, Rossetto T, Costa A (2012) Cyclic response of RC beam–column joints reinforced with plain bars: an experimental testing campaign. In: Proceedings of 15th world conference on earthquake engineering, Lisbon, Portugal



- Murty CVR, Rai D, Bajpai KK, Jain SK (2003) Effectiveness of reinforcement details in exterior reinforced concrete beam–column joints for earthquake resistance. *ACI Struct J* 100(2):149–156
- Niroomandi A, Maheri A, Maheri MR, Mahini SS (2010) Seismic performance of ordinary RC frames retrofitted at joints by FRP sheets. *Eng Struct* 32:2326–2336
- Niroomandi A, Najafgholipour MA, Ronagh HR (2014) Numerical investigation of the affecting parameters on the shear failure of nonductile RC exterior joints. *Eng Failure Anal* 46:62–67
- NZS 3101 (1995) Design of concrete structures, vols 1, 2. Standards Association of New Zealand, Wellington
- Pampanin S, Calvi GM, Moratti M (2002) Seismic behavior of RC beam–column joints designed for gravity only. In: *Proceeding, 12th European conference on earthquake engineering (ECEE)*, London
- Pampanin S, Magenes G, Carr A (2003) Modelling of shear hinge mechanism in poorly detailed RC beam–column joints. In: *Fib symposium on concrete structures in seismic regions*, Athens, Greece
- Pampanin S, Bolognini D, Pavese A (2007) Performance-based seismic retrofit strategy for existing RC frame systems using FRP composites. *J Compos Constr* 11(2):211–226
- Pantelides CP, Hansen J, Nadauld J, Revealey LD (2002) Assessment of reinforced concrete building exterior joints with substandard details. Report no. PEER 2002/18. Pacific Earthquake Engineering Research Center
- Park S, Mosalam KM (2012) Parameters for shear strength prediction of exterior beam–column joints without transverse reinforcement. *Eng Struct* 36:198–209
- Parvin A, Altay S, Yalcin C, Kaya O (2010) CFRP Rehabilitation of concrete frame joints with inadequate shear and anchorage details. *J Compos Constr* 14(1):72–82
- Priestley MJN (1997) Displacement based seismic assessment of reinforced concrete buildings. *J Earthq Eng* 1(1):157–192
- Priestley MJN, Seible F, Calvi GM (1996) *Seismic design and retrofit of bridge structures*. Wiley, New York
- Realfonzo R, Napoli A, Pinilla JGR (2014) Cyclic behavior of RC beam–column joints strengthened with FRP systems. *Constr Build Mater* 54:282–297
- Ricci P, De Risi MT, Verderame GM, Manfredi G (2016) Experimental tests of unreinforced exterior beam–column joints with plain bars. *Eng Struct* 118:178–194
- Santarsiero G, Masi A (2015) Seismic performance of RC beam–column joints retrofitted with steel dissipation jackets. *Eng Struct* 85:95–106
- Sasmal S (2009) Performance evaluation and strengthening of deficient beam–column sub-assemblages under cyclic loading. Ph.D. Dissertation. University of Stuttgart, Stuttgart
- Sezen H (2002) Seismic behavior and Modelling of reinforced concrete building columns. Ph.D. Dissertation. University of California, Berkeley, California
- Shafaei J, Zareian MS, Hosseini Marefat MS (2014) Effects of joint flexibility on lateral response of reinforced concrete frames. *Eng Struct* 81:412–431
- Sharma A (2013) Seismic behavior and retrofitting of RC frame structures with emphasis on beam–column joints: experiments and numerical Modelling. Ph.D. Dissertation. University of Stuttgart, Stuttgart
- Sharma A, Eligehausen R, Reddy GR (2011) A new model to simulate joint shear behavior of poorly detailed beam–column connections in RC structures under seismic loads, part I: exterior joints. *Eng Struct* 33:1034–1035
- Shayanfar J, Akbarzadeh BH (2016) Numerical model to simulate shear behaviour of RC joints and columns. *Comput Concrete* 18(4):877–901
- Shayanfar J, Akbarzadeh BH (2017) Nonlinear analysis of RC frames considering shear behaviour of members under varying axial load. *Bull Earthq Eng* 15(5):2055–2078
- Shayanfar J, Akbarzadeh BH (2018) A practical model for simulating nonlinear behaviour of FRP strengthened RC beam–column joints. *Steel Compos Struct* 27(1):49–74
- Shayanfar J, Akbarzadeh BH, Niroomandi A (2016) A proposed model for predicting nonlinear behavior of RC joints under seismic loads. *Mater Des* 95:563–579
- Shayanfar J, Shamkhali MH, Akbarzadeh BH, Hemmati A, Mirani SS (2017) Simulation of nonlinear behaviour of RC joints with 180°-hook under varying axial load. In: *The international conference on recent progresses in civil engineering*, Amol
- Shayanfar J, Akbarzadeh BH, Parvin A (2018) Analytical prediction of seismic behavior of RC joints and columns under varying axial load. *Eng Struct* 174:792–813
- Shrestha R, Smith ST, Samali B (2009) Strengthening RC beam–column connections with FRP strips. *Proc Inst Civil Eng Struct Build* 162(5):323–334
- Tsonos AG (2002) Seismic repair of exterior R/C beam-to-column joints using two sided jackets. *Struct Eng Mech* 13(1):17–34
- Tsonos AG (2007) Cyclic load behavior of reinforced concrete beam–column subassemblages of modern structures. *ACI Struct J* 104(4):468

- Tsonos AG (2014) An innovative solution for strengthening old R/C structures and for improving the FRP strengthening method. *Struct Monit Maint Int J* 1(3):323–338
- Tsonos AG, Papanikolaou KV (2003) Post-earthquake repair and strengthening of reinforced concrete beam–column connections (theoretical & experimental investigation). *Bull N Z Soc Earthq Eng* 36(2):73–93
- Tsonos AG, Tegos IA, Penelis GG (1992) Seismic resistance of type 2 exterior beam–column joints reinforced with inclined bars. *ACI Struct J* 89(1):3–12
- Unal M, Burak B (2013) Development and analytical verification of an inelastic reinforced concrete joint model. *Eng Struct* 52:284–294
- Wong HF (2005). Shear strength and seismic performance of non-seismically designed reinforced concrete beam–column joints. Ph.D. dissertation, Hong Kong Univ of Science and Technology, Kwoloon, Hong Kong
- Wong HF, Kuang JS (2008) Effects of beam: column depth ratio on joint seismic behaviour. *Proc Inst Civil Eng Struct Build* 161(2):91–101
- Yurdakul O, Avsar O (2016) Strengthening of substandard reinforced concrete beam–column joints by external post-tension rods. *Eng Struct* 107:9–22